



# DEFENSE TECHNICAL INFORMATION CENTER

*Information for the Defense Community*

DTIC<sup>®</sup> has determined on 28/12/2009 that this Technical Document has the Distribution Statement checked below. The current distribution for this document can be found in the DTIC<sup>®</sup> Technical Report Database.

**DISTRIBUTION STATEMENT A.** Approved for public release; distribution is unlimited.

**© COPYRIGHTED;** U.S. Government or Federal Rights License. All other rights and uses except those permitted by copyright law are reserved by the copyright owner.

**DISTRIBUTION STATEMENT B.** Distribution authorized to U.S. Government agencies only (fill in reason) (date of determination). Other requests for this document shall be referred to (insert controlling DoD office)

**DISTRIBUTION STATEMENT C.** Distribution authorized to U.S. Government Agencies and their contractors (fill in reason) (date of determination). Other requests for this document shall be referred to (insert controlling DoD office)

**DISTRIBUTION STATEMENT D.** Distribution authorized to the Department of Defense and U.S. DoD contractors only (fill in reason) (date of determination). Other requests shall be referred to (insert controlling DoD office).

**DISTRIBUTION STATEMENT E.** Distribution authorized to DoD Components only (fill in reason) (date of determination). Other requests shall be referred to (insert controlling DoD office).

**DISTRIBUTION STATEMENT F.** Further dissemination only as directed by (inserting controlling DoD office) (date of determination) or higher DoD authority.

*Distribution Statement F is also used when a document does not contain a distribution statement and no distribution statement can be determined.*

**DISTRIBUTION STATEMENT X.** Distribution authorized to U.S. Government Agencies and private individuals or enterprises eligible to obtain export-controlled technical data in accordance with DoDD 5230.25; (date of determination). DoD Controlling Office is (insert controlling DoD office).

DEVELOPMENT OF DATA-ASSIMILATION-QUALITY MODIS  
AND MISR OVER OCEAN AEROSOL PRODUCTS

by

Yingxi Shi  
Bachelor of Science, Sun Yat-sen University, 2006

A Thesis  
Submitted to the Graduate Faculty

of the

University of North Dakota

in partial fulfillment of the requirements

for the degree of

Master of Science

Grand Forks, North Dakota  
August  
2009

**20091223185**

Copyright 2009 Yingxi Shi

This thesis, submitted by Yingxi Shi in partial fulfillment of the requirements for the Degree of Master of Science from the University of North Dakota, has been read by the Faculty Advisory Committee under whom the work has been done and is hereby approved.

---

Chairperson

---

---

---

---

This thesis meets the standards for appearance, conforms to the style and format requirements of the Graduate School of the University of North Dakota, and is hereby approved.

---

Dean of the Graduate School

---

Date

PERMISSION

Title           Development of Data-Assimilation-Quality MODIS and MISR Over  
                  Ocean Aerosol Products

Department    Atmospheric Sciences

Degree         Master of Science

In presenting this thesis in partial fulfillment of the requirements for a graduate degree from the University of North Dakota, I agree that the library of this University shall make it freely available for inspection. I further agree that permission for extensive copying for scholarly purposes may be granted by the professor who supervised my thesis work or, in his absence, by the chairperson of the department or the dean of the Graduate School. It is understood that any copying or publication or other use of this thesis or part thereof for financial gain shall not be allowed without my written permission. It is also understood that due recognition shall be given to me and to the University of North Dakota in any scholarly use which may be made of any material in my thesis.

Signature \_\_\_\_\_

Date \_\_\_\_\_

## TABLE OF CONTENTS

LIST OF FIGURES .....	vii
LIST OF TABLES .....	ix
ACKNOWLEDGEMENTS .....	x
ABSTRACT .....	xi
CHAPTER	
1.    INTRODUCTION .....	1
II.   BACKGROUND .....	3
Aerosol Sources and Physical Properties .....	3
Aerosol Global Distribution .....	4
Aerosol Climate Impacts .....	7
Aerosol Direct and Indirect Climate Effects .....	7
Aerosol Impacts on Atmospheric Circulation .....	9
Aerosol Impacts on Air Quality .....	9
Aerosol Impacts on Visibility .....	10
III.  MOTIVATION .....	11
Traditional Methods in Aerosol Measurements .....	11
In Situ Measurement .....	11
Ground Based Measurement .....	11
Remotely Sensed Data from Space .....	12
Motivation .....	13

IV.	DATA .....	16
	MODIS and Algorithm .....	16
	MISR and Algorithm .....	19
	AERONET and Algorithm .....	20
	NOGAPS Wind Speed Data .....	22
V.	UNCERTAINTY ANALYSIS .....	23
	Collocation Methods .....	23
	Sources of Uncertainties .....	25
	Lower Boundary Condition .....	25
	Cloud Contamination and Cloud Artifacts .....	27
	Microphysical Properties .....	32
VI.	RESULTS AND DISCUSSIONS .....	40
	Empirical Corrections .....	41
	Quality Assurance Analysis .....	44
	Validation .....	45
	Independent Validation.....	50
	Spatial Evaluation.....	50
	Sensitivity Study .....	52
VII.	CONCLUSION AND FUTURE STUDY .....	54
	REFERENCES .....	56

## LIST OF FIGURES

Figure		Page
1.	Seasonal aerosol distribution using $\tau_{0.55}$ from the MODIS Terra Collection 5 aerosol products for 2005 .....	5
2.	Global aerosol fine mode fraction ( $\eta$ ) distribution using $\eta$ from the MODIS Terra Collection 5 aerosol products for 2005 .....	7
3.	Scatter plots of MISR vs. MODIS coincident, mid-visible $\tau$ for January 2006, contoured using a fractional power-law color scale to show the range of point densities. ....	14
4.	Scatter plots of the level 1.5 versus level 2.0 AERONET $\tau_{0.55}$ for 2005 .....	22
5.	AERONET minus MODIS Terra $\tau_{0.87}$ versus NOGAPS near-surface wind speed .....	28
6.	MODIS Terra versus AERONET level 2.0 $\tau_{0.87}$ as function of cloud fraction for the year 2005 .....	30
7.	MODIS Terra versus AERONET level 1.5 $\tau_{0.87}$ as a function of cloud fraction for the year 2005-2007 .....	31
8.	MISR versus AERONET level 1.5 $\tau_{0.87}$ as a function of cloud fraction for the year 2005 and 2006 .....	32
9.	Terra MODIS versus AERONET $\tau_{0.55}$ for two ranges of $\eta$ based on AERONET $\eta_{sp}$ . ....	34
10.	Scatter plot of the MODIS fine mode fraction and AERONET-derived fine mode fraction at the 0.55 $\mu\text{m}$ wavelength .....	35
11.	Slope of MODIS versus AERONET level 2.0 $\tau$ as function of cloud fraction and two fine mode fraction from AERONET for the year 2005 .....	37
12.	Slope of MODIS versus AERONET level 1.5 $\tau$ as function of cloud fraction and two fine mode fraction from AERONET for 2005-2007 .....	38
13.	Microphysical effects on MISR aerosol products .....	39

14.	Data Processes Flow Chart .....	40
15.	Scatter plot of standard error of $\tau$ versus $\tau$ .....	45
16.	Scatter plot of the Terra MODIS versus AERONET level 2.0 $\tau_{0.55}$ for 2005 .....	47
17.	Scatter plot of the Terra MODIS versus AERONET level 2.0 $\tau_{0.55}$ for 2007 .....	48
18.	Scatter plot of the MISR versus the AERONET level 1.5 $\tau_{0.558}$ for 2005 .....	49
19.	Spatial distribution of $\tau$ .....	51

## LIST OF TABLES

Table	Page
1. Coefficients for Terra and Aqua as A Function of Glint Angle ( $\psi$ ) for (6.2) .....	42
2. Coefficients for (6.3).....	43
3. Sensitivity studies of the empirical corrections and quality assurance procedures of Terra MODIS Collection 5 and the AERONET Level 2.0 Aerosol Products.....	53

## ACKNOWLEDGEMENTS

I would like to express my sincere gratitude to my advisor, Dr. Jianglong Zhang, for his guidance during my research and study, for his patience, motivation, enthusiasm and expertise. I could not have imagined having a better advisor for my master research. Besides my advisor, I would like to thank the rest of my advising committee of Xiquan Dong, Mark A. Askelson, and Christina N. Hsu for their encouragement, insightful comments and support.

I would like to thank all the faculties and graduate students in the Atmospheric Sciences Department, especially Prof. David Delene, Aaron Kennedy, Hongchun Jin, and Zhe Feng, for their technical supports from IDL programming to fixing computer failures, for the stimulating discussions, and for helping through the late night homework sessions.

This research is supported by Office of Naval Research (ONR) Code 322, and the ONR YIP program. I thank Drs. Lorraine. A. Remer, Ralph A. Kahn, and Thomas F. Eck for their suggestions on my research and for the use of their data (MODIS, MISR and AERONET).

Last but not the least, I would like to thank my family and Jeffrey Kuntz for believing in me and for always being there.

## ABSTRACT

Aerosol related researches have gained a significant amount of attention over the past decade, largely due to its importance in climate change studies. In addition, aerosols are also heavily studied for air quality and visibility forecasts, using Chemical Transport Models (CTM). Studies have shown that the CTM's aerosol forecasting capability can be significantly improved through the assimilation of satellite based aerosol measurements. However, large uncertainties and disagreements frequently exist in these satellite aerosol products. Thus, it is critical to have quality control and quality assurance procedures before assimilating these observations into numerical models.

Uncertainties in the over-water aerosol optical depth (AOD) from Moderate Resolution Imaging Spectroradiometer (MODIS, collection 5) and the Multiangle Imaging SpectroRadiometer (MISR, version 22) aerosol products were examined as functions of observing conditions, such as surface characteristics, aerosol optical properties, and cloud artifacts. Empirical corrections and quality assurance procedures were developed. After applying these empirical correction and quality assurance steps the uncertainties in the MISR AOD are reduced by 10% and 17%, respectively, with a maximum regional reduction of 50% over the southern oceans. A sensitivity study was conducted and quality-assured level 3 MODIS and MISR over water aerosol products were produced. The newly developed MODIS and MISR over water aerosol products will be used in future aerosol data assimilation and aerosol climatology studies,

and will also be useful to other researchers who are using the MODIS and MISR satellite products in their projects.

## CHAPTER 1

### INTRODUCTION

Climate change is becoming a mainstream issue as recent observations have shown an alarming surface temperature increase during the past 100 years (Kaufman et al., 2002). Scientists believe that man-made greenhouse gases are the primary driving forces behind global warming. The estimated warming effects reach  $2.63 \pm 0.26$  watts per meter square ( $\text{W m}^{-2}$ ) from long-lived greenhouse gases such as carbon dioxide ( $\text{CO}_2$ ), methane ( $\text{CH}_4$ ), nitrous oxide ( $\text{N}_2\text{O}$ ), non-methane halocarbons (NMHC), and sulfur hexafluoride ( $\text{SF}_6$ ) (IPCC 2007). However, recent studies have shown that forcing from aerosols could have a similar climatic impact as green house gases, yet opposite in sign (IPCC 2007).

Aerosols are suspended particles in the atmosphere of Earth whose spatial distributions largely depend on their source regions and atmospheric circulation patterns throughout the boundary layer. Aerosols directly affect climate by cooling the Earth's surface and indirectly by changing cloud properties, as well as impact air quality (e.g. Wang and Christopher, 2003) and visibility (e.g. Appel et al., 1985). Studies have found that aerosols could potentially alter general circulation patterns (e.g. Kim et al., 2006) and significantly influence both local and regional climates (e.g. Venkataraman et al., 2005; Kaufman and Fraser, 1997). As a consequence of their critical roles in the ecosystem of Earth, aerosol related phenomena have been heavily studied for the past two decades.

Aerosols are measured through various means including ground-based, *in situ* and space-borne observations. Because of the high spatial and temporal variations in aerosol properties, space-borne aerosol sensors are the only means by which daily observations can be obtained on a global scale. However, biases and uncertainties exist in satellite aerosol data due to the complications inherent to retrieval processes and varying observational conditions (e.g. Liu and Mishchenko, 2008). Therefore, it is necessary to have a comprehensive understanding and careful documentation of those uncertainties before using such data in scientific applications, such as aerosol forecasting through data assimilation.

## CHAPTER II

### BACKGROUND

A brief introduction of aerosols is presented in this chapter. Aerosol characteristics such as their sources, physical properties, global distribution, and their climate impacts are discussed.

#### Aerosol Sources and Physical Properties

Aerosols originate from both natural and anthropogenic sources. Examples of natural aerosols include windblown mineral dust from deserts, smoke plumes from natural forest fires, sulfate aerosols and ashes from volcanic eruptions, sea salt aerosols from bursting bubbles over the ocean surface (O'Dowd et al., 1997), and sulfate aerosols that are derived from oceanic dimethyl sulfide (DMS) released from phytoplankton (Andreae, 2007). Examples of anthropogenic aerosols include pollutants from fossil fuel combustion, dust generated from perturbed soil due to land usage, and aerosols from agricultural fires (e.g. biomass burning).

Beside their sources, aerosols are also categorized based on their size. Theoretically, aerosols can be categorized into Aitken particle with diameters from 0.001 to 0.1  $\mu\text{m}$ , large particle with diameters from 0.1 to 1  $\mu\text{m}$ , and giant particle with diameters from 1 to 10  $\mu\text{m}$  (Peixoto and Oort, 1992). In practice, two aerosol types are commonly studied: (1) large mode aerosols such as dust and sea salt which have diameters greater than 2  $\mu\text{m}$  and (2) fine mode particles like pollution and smoke which are submicron in size and have diameters smaller than 1  $\mu\text{m}$  (Whitby, 1978).

Particle size is a dominant factor in determining the residence time of aerosols. Generally, smaller particles are more likely to stay suspended in the air longer than larger particles. Although most aerosols have residence time periods ranging from days to weeks (Cooke and Wilson, 1996), some aerosol particles can remain in the free troposphere and/or stratosphere for several months and even up to a year and can travel a long distance. For example, a recent study traced a windblown dust episode that began on 7 April 2006 and originated in Inner-Mongolia. The dust traveled across the Pacific Ocean and made its way to the west coast of the United States after ten days (Obrecht, 2008). Similarly, volcanic eruptions can send aerosols into the stratosphere where they are distributed as a thin layer around the Earth that can persist for more than a year and affect the climate (Brock et al., 1993).

#### Aerosol Global Distribution

Figure 1 shows the global and seasonal distributions of aerosol optical depth (AOD, denoted as  $\tau$ ) at  $0.55\mu\text{m}$ .  $\tau$  is defined as the integrated light attenuation throughout the entire column of air. Figure 1 was generated using the MODIS Terra Collection 5 (explained in CHAPTER IV) over ocean aerosol products by averaging  $\tau$  for each degree of latitude and longitude over the year 2005 for each of the four seasons.

High aerosol loadings are found year round over the Saharan Desert and the western coast of North Africa, as well as in East and South Asia (e.g., the Indian Peninsula) and the nearby Pacific Ocean (Fig. 1). Figure 1 also shows the variations of aerosol concentrations over both the northern and southern hemispheres. The Northern Hemisphere spring (March, April, May, or MAM) is the typical season for East Asian dust storms. Figure 1b shows that the aerosol loading peaks over the east coast of China

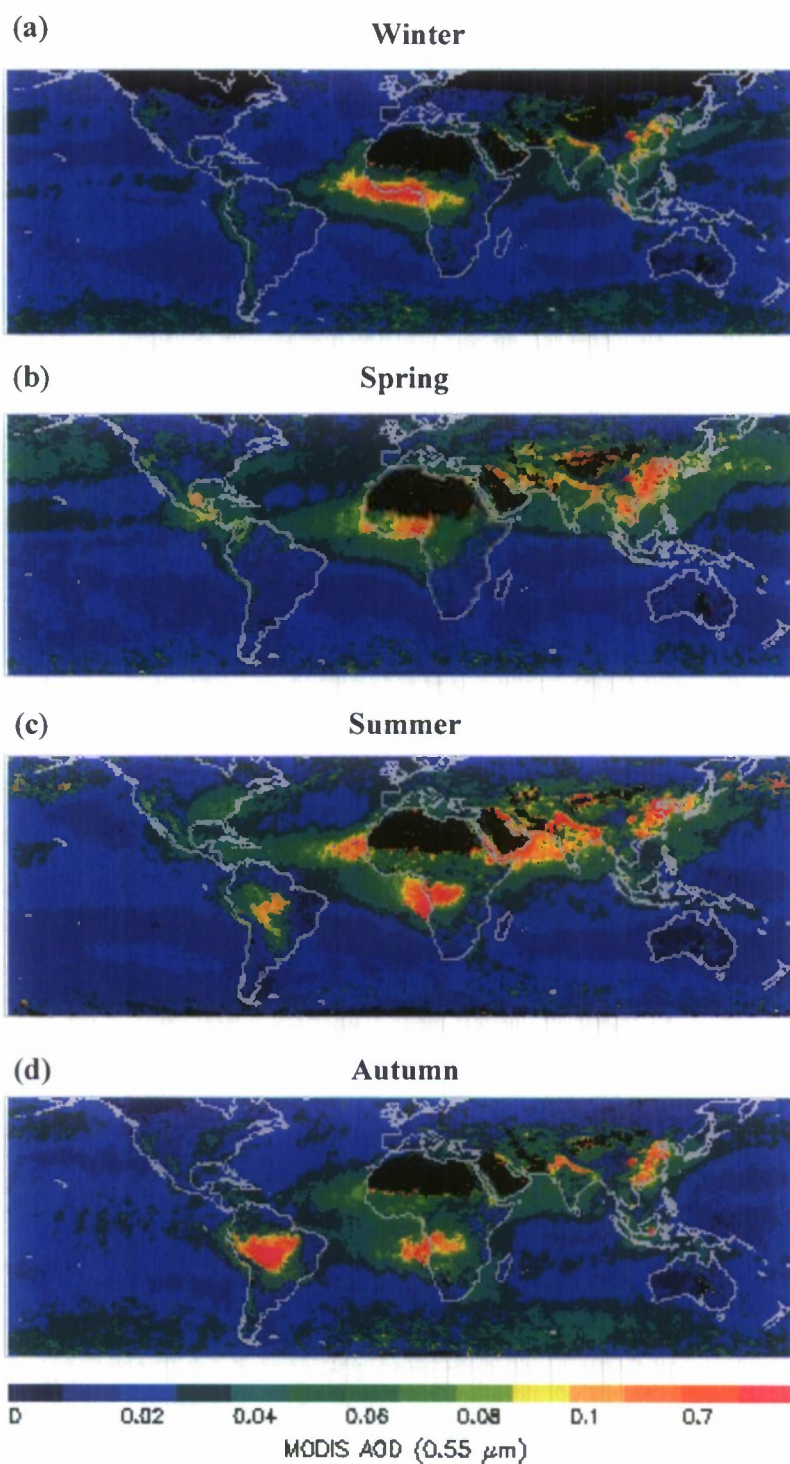


Figure 1. Seasonal aerosol distribution using  $\tau_{0.55}$  from the MODIS Terra Collection 5 aerosol products for 2005. (a) Winter (December, January and February); (b) Spring (March, April and May); (c) Summer (June, July and August); (d) Autumn (September, October and November).

and extends across the Pacific Ocean. Central America is another region with high  $\tau$  values due to farmers setting fires to rainforests in order to clear land for agricultural purposes (Koren et al., 2004). During the Northern Hemisphere summer (June, July, August, or JJA), high aerosol concentrations are found over both South America and South Africa due to a similar reason as for Central America, where a significant amount of aerosols is released due to the biomass burning as a result of land clearing (Roberts et al., 2008). During the Northern Hemisphere fall (September, October and November, or SON), the increased biomass burning in South America, South Africa and Australia results in high  $\tau$  values in the Southern Hemisphere.

Figure 2 shows the global distribution of the aerosol fine mode fraction ( $\eta$ ).  $\eta$  is the ratio of the fine mode  $\tau$  to the total  $\tau$ , which can be used as a proxy for aerosol particle size. Small  $\eta$  values represent coarse mode particles such as dust and sea salt, whereas large  $\eta$  values can be a proxy for fine mode particles such as smoke and pollutant aerosols (Remer et al., 2005). Figure 2 was created by averaging  $\eta$  at every one latitude and longitude bin for 2005 using the same products used in generating Fig.1.

Annually, the main source regions for fine mode aerosols are located at Central and South America, South Africa, and the South Asian islands (e.g. Indonesia) as a result of biomass burning, as well as the east coast of the United States, Europe and Asia, due to pollutions. Coarse particle source areas are associated with deserts, such as the Saharan desert.

### MODIS Aerosol Fine Mode Fraction Distribution

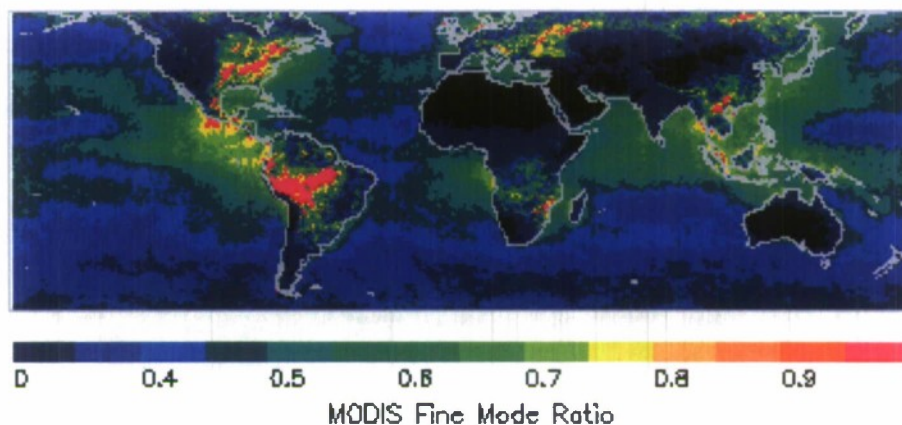


Figure 2. Global aerosol fine mode fraction ( $\eta$ ) distribution using  $\eta$  from the MODIS Terra Collection 5 aerosol products for 2005

#### Aerosol Climate Impacts

Aerosols affect climate directly by attenuating sunlight and indirectly by modifying cloud properties. Aerosols also affect climate by changing regional precipitation patterns and altering global atmospheric circulations.

#### *Aerosol Direct and Indirect Climate Effects*

Aerosols directly affect climate by altering the Earth's radiation budget. Highly reflective aerosols increase the Earth's planetary albedo and thereby reflect more solar energy back to space, thus cooling the Earth. Additionally, absorbing aerosols, like black carbon particles present in urban haze and smoke from biomass burning, can absorb solar energy, thus heating the atmosphere. Bellouin et al. (2005) estimated the direct aerosol radiative forcing of aerosols at the top of the atmosphere under clear-sky conditions to be  $-1.9 \text{ W m}^{-2}$  per year globally with an uncertainty of  $\pm 0.3 \text{ W m}^{-2}$ . This amount of forcing could counteract a significant portion of warming effects associated with the greenhouse gases ( $2.63 \pm 0.26 \text{ W m}^{-2}$ ).

Aerosols indirectly affect climate by modifying cloud radiative properties such as cloud drop size, cloud lifetime, and albedo (Nakajima et al., 2001). Aerosols can serve as cloud condensation nuclei (CCN), which are “cores” in cloud droplet formation. Studies have found that increasing aerosol concentration could lead to an increase in cloud droplet concentration, which in turn decreases cloud particle size (Hobbs and Radke, 1969; Ramanathan et al., 2001). Some studies (Squires, 1958; Gunn and Phillips, 1957) have suggested that a decrease in cloud droplet size can reduce the chance of droplet-collision, which further prevents cloud droplets from reaching the critical size needed to form precipitation. Thus, aerosols can extend cloud lifetime and change the energy budget of Earth (Albrecht, 1989). Moreover, the smaller sizes of cloud droplets and concomitant increased number concentrations lead to increases in cloud albedo that can further cool the atmosphere (Andreae et al., 2005). All of these aerosol indirect effects are caused by modifying cloud microphysical processes and are considered as the first indirect aerosol effect.

Aerosols can also change the geographical coverage of clouds and precipitation, which is known as secondary aerosol indirect effect (Kaufman et al., 2002). Studies have suggested that the capability of aerosols to absorb solar radiation could warm the atmosphere and dissipate clouds (Koren et al., 2004). Other studies have found that biomass-burning-generated aerosols over the Amazon basin could suppress cumulus cloud formation (Koren et al., 2004). However, the effects of aerosols on precipitation are less clear even though several studies have sought to examine this issue from both observational and model based methods (Kaufman et al., 2005; Zhang and Reid, 2006).

### *Aerosol Impacts on Atmospheric Circulation*

By altering the global energy balance, aerosols can impact regional and global atmospheric circulations. For example, the absorption of radiation by dust over the Sahara desert warms the atmosphere. Air rises in the Saharan region and falls over Southern Europe, advecting dry and warm weather in the process (Kim et al., 2006). Strong atmospheric heating from aerosols also alters the monsoon patterns in India and China. This influences the major water source by modifying precipitation patterns for those regions during the summer (Lau et al., 2006). High dust loading combined with the presence of absorbing aerosols over the northern and southern slopes of the Tibetan Plateau (TP) results in enhanced absorption of solar radiation. The resulting anomalously high temperatures in the middle to upper troposphere on the southern slopes of the TP bring earlier and enhanced precipitation to India while it suppresses rainfall in Eastern Asia. Aerosols not only affect regional air circulations but also global ones. For instance, Zhang et al. (2007) found that Asian pollution could intensify the Pacific storm track, which plays an important role in global meridional heat transport.

### *Aerosol Impacts on Air Quality*

Aerosol particles, especially particles with sizes less than 2.5  $\mu\text{m}$  (PM<sub>2.5</sub>) are major sources of air pollution. Submicron sized aerosols can be inhaled into lungs, remain in lung parenchyma (Churg and Brauer, 1997), and induce inflammation in bronchioles (Tong et al., 2006). Studies have shown that short time exposure to polluted air causes health problems like cardiovascular and respiratory diseases, especially in children and the elderly (Brunekreef et al., 2000). Long-term exposure to high particle

concentrations has been associated with problems such as lung cancer and the development of chronic bronchitis, and even premature death (Krewski et al., 2005).

#### *Aerosol Impacts on Visibility*

Aerosols also reduce visibility by absorbing and scattering of light (Dzubay et al., 1982). For example, during dust storms or heavy biomass burning events, visibility is severely reduced. In a clear atmosphere, the visual range can reach 200-300 km horizontally. Studies have shown that during heavy aerosol episodes, the visual range could be limited to a few kilometers or less (Dzubay et al., 1982). Understanding the impact of aerosols on visibility is important as it can affect the safety of ground, sea, and air traffic (Bäumer et al., 2008).

## CHAPTER III

### MOTIVATION

#### Traditional Methods in Aerosol Measurements

Traditionally, aerosol physical and optical properties are measured through three basic methods: (1) *in situ*, (2) ground-based, and (3) remote sensing. The advantages and disadvantages of each method are discussed here.

#### *In Situ Measurement*

An *in situ* measurement is the direct measurement of aerosol properties at the location of interest. During field experiments, aerosol properties such as size distribution, shape, chemical composition, and radiative properties are commonly measured--usually with aircraft. This method provides reliable, first hand data and serves as benchmarks for other aerosol studies such as modeling studies. However, *in situ* measurements are often costly, and are limited to specific time frames and fixed locations. Thus, *in situ* measurements cannot provide the whole picture of global aerosol distribution, or provide a data set for climatology studies that require long term observations.

#### *Ground Based Measurement*

Ground based measurements provide continuous observations over long periods of time. The AErosol RObotic NETwork (AERONET) is an example of this type of measurement and comprises a global network of sites (Holben et al., 1998). In the ground based method, direct measurements of solar radiation attenuated by aerosols at

specified wavelengths are obtained. Aerosol information can then be derived from the observed radiance through an inversion technique (Holben et al., 1998). Thus, ground-based measurements can provide long-term observations over numerous surface sites. Although there are some uncertainties exist due to calibrations, observation environments, and the retrieval processes, these uncertainties are much less than satellite retrievals. Therefore, the ground-based observations can be served as ground truth to validate satellite retrievals. Finally the validated satellite retrievals can be used to study the global coverage and distribution of aerosol properties. However, one site can only measure a limited area of the Earth, therefore making it impossible to have global coverage with this method.

#### *Remotely Sensed Data from Space*

Satellites detect and receive reflected shortwave radiation from the Earth's surface and from components of the atmosphere. This radiation contains the integrated information regarding surface and atmospheric properties. Therefore, it is necessary to develop retrieval algorithms to identify the surface and atmosphere contribution from the integrated reflection. The optical properties and sizes of aerosols then can be retrieved from satellite observed radiance based on their sensitivities to different wavelength, angularity and polarization. The spectral, temporal, spatial and radiometric resolutions of satellites determine the number and sizes of spectral regions in which the sensor records data, the time span for revisiting the same area, the size of the field of view, and the sensitivity of detectors to small differences in electromagnetic energy. Satellites have different advantages in terms of measuring aerosols and using various combinations of

these four resolutions helps solve the different problems associated with aerosol property retrievals.

### Motivation

Compared to *in situ* and ground-based observations, remotely-sensed space-borne observations are the only means by which daily measurements on a global scale can be achieved. For this reason, satellite aerosol products are widely used in the scientific community for various applications, such as aerosol climate forcing studies, air quality studies, and aerosol data assimilation studies (Kaufman et al., 2002). However, recent studies have shown that large uncertainties exist in the current satellite aerosol products (e.g. Liu and Mishchenko, 2008). For example, Fig. 3 (Kahn et al., in press) shows the inter-comparisons between collocated MODIS/Terra Collection 5 & MISR Version 22 aerosol products (explained in CHAPTER IV). Similar results were also reported by Liu and Mishchenko (2008). For the over land comparisons, a correlation of 0.7 is found between the two aerosol products, and pixels are grouped around roughly three axes that radiate outward from the origin. This indicates that under certain conditions, the retrieval methods are significantly different for the two products, which leads to disagreements in the satellite retrieved aerosol properties (Kahn et al., in press).

For the over ocean comparisons, a correlation of 0.9 is found, indicating the quality of these products is much better than those over land (Fig. 3). This is understandable since surface reflectivity is a key parameter in satellite aerosol retrievals, and thus better performance is expected over a relatively uniform, dark ocean surface (Tanré et al., 1997). However, large scatter is also found in Fig. 3a, especially for high  $\tau$  samples. In general, MODIS  $\tau$  values are higher than those obtained from MISR.

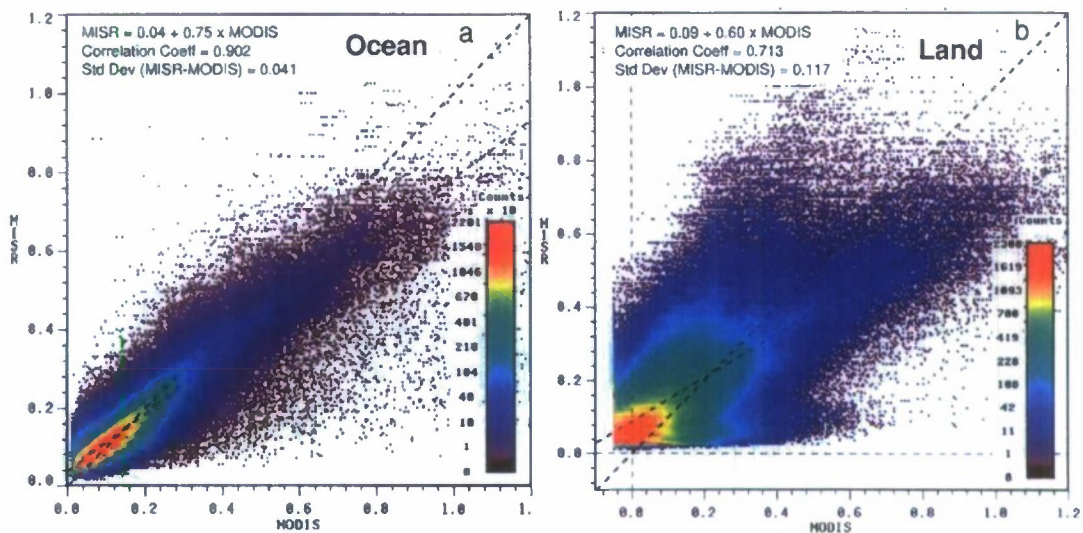


Figure 3. “Scatter plots of MISR vs. MODIS coincident, mid-visible  $\tau$  for January 2006, contoured using a fractional power-law color scale to show the range of point densities. (a) All over-ocean grid points. (b) All over-land grid points. For these plots, MISR Standard aerosol products Version 22, and MODIS/Terra Collection 5 data were used. The regression-line fits, correlation coefficients, and standard deviations are given in the upper left of each plot” (Kahn et al., in press).

Furthermore, other studies have reported that large uncertainties could exist in the over ocean aerosol products, especially for certain observing conditions such as in the vicinity of clouds (Zhang et al., 2005a), near glint regions (Kaufman et al., 2002), and over regions with high near surface wind (Zhang and Reid, 2006).

The large uncertainties in satellite aerosol retrievals could limit the use of these products in aerosol related studies, especially for studies involving aerosol data assimilation. Aerosol data assimilation is the process of integrating observational data into chemical transport models (CTM). Studies have suggested that the accuracy of CTM-based aerosol forecasting could be improved if satellite observations are used in the data assimilation and numerical models (Zhang et al., 2008). However, aerosol forecast accuracy is highly dependent upon the quality of the input observational data. Without

carefully studying and identifying associated uncertainties, incorporating such products into models could potentially degrade a model's performance. These factors motivate both further comprehension of characteristics of these satellite products and the development of reliable data sets suitable for studies that depend upon improved data accuracy.

Efforts have been directed towards identifying and removing noise and bias in satellite aerosol data. For example, Zhang and Reid (2006) studied uncertainties associated with the MODIS Collection 4 (explained in CHAPTER IV) over ocean aerosol products, and derived a quality assured satellite aerosol product that has reduced uncertainties. Over land corrections are much more complicated due to the high variability of land surface properties (Hyer et al., in submission). Due to this complexity of land surface properties, only satellite retrievals over ocean were investigated using the MODIS Collection 5 over ocean aerosol products and the MISR Version 22 aerosol products and the over land products will be studied as future work. Empirical correction procedures and quality checks were developed and applied to create new aerosol products for future aerosol data assimilation studies.

## CHAPTER IV

### DATA

Four data sets are used in this study: (1) MODIS Collection 5 aerosol data, (2) MISR Version 22 aerosol data, (3) AERONET data, and (4) NOGAPS modeled wind speed data. MODIS has high spatial resolution, wide spectral range, and most importantly, full global coverage almost twice a day, which provides detailed information about aerosol evolution within a short time interval. MISR has nine different observing angles ranging from -70 to 70 degrees, which enables the measurements of reflected energy from both the surface and the atmosphere as a function of observing angle, and is especially useful for aerosol retrievals at high surface albedo conditions. AERONET data are considered as the validation benchmark for the two satellite aerosol products. Details regarding these four data sets are provided below.

#### MODIS and Algorithm

On board both Terra (equator overpass time 10:30 AM local standard time) and Aqua (equator overpass time 1:30 PM local standard time) satellites, the Moderate Resolution Imaging Spectroradiometer (MODIS), with a high spatial resolution of 250-1000 meters, a 2330 km swath, and a total of 36 spectral channels, provides observations twice a day that cover most of the planet. Six wavelengths, ranging from 0.47 to 2.13  $\mu\text{m}$ , are used to retrieve aerosol optical properties and generate the "level 2.0" aerosol products. Level 2.0 MODIS aerosol products have a spatial resolution of 10 kilometers.

Validated against AERONET data, the averaged uncertainties of the MODIS  $\tau$  products are  $0.03 \pm 0.05\tau$  over ocean and  $0.05 \pm 0.15\tau$  over land (Remer et al., 2005).

After the first version (Collection 1) of the MODIS aerosol product made available to the scientific community in 2000, changes and improvements have been made to the original MODIS aerosol retrieving algorithms (Kaufman et al., 1997a; Tanré et al., 1997), and new versions of the MODIS aerosol products have been released for public access. The most current version is the MODIS Collection 5 (Remer et al., 2005). Two Collection 5 MODIS aerosol products, the Terra MODIS (MOD04) and Aqua MODIS (MYD04) aerosol products were used in this study. Note that different retrieval algorithms are used for over land and over ocean, and only over ocean algorithms are concerned and explained.

Over the ocean, aerosol optical properties are retrieved through a Look Up Table (LUT) approach following three steps. First, a radiative transfer model is used to calculate satellite radiances over all seven wavelengths as functions of pre-determined observing conditions and aerosol models. These radiances form the LUT. Then, the satellite observed spectral radiances are used to match the LUT calculated radiances until approaches a minimum difference between the measured radiances and the LUT radiances. Finally, the aerosol model values from step 2 are considered as the first order solution and the aerosol parameters from the selected aerosol models are used to calculate aerosol properties such as aerosol optical depth.

In the current over ocean retrieval algorithm, four pre-determined aerosol models are used for small mode aerosols (such as sulfate aerosols) and five are used for large mode aerosols (Remer et al., 2005), which is one fewer for both categories compared to

the original algorithm (Tanré et al., 1997). The current retrieval algorithm reduces the sensitivity of step 2 to calibration errors. Because a calibration shift, which is an increase of 0.015 in  $\tau$ , has been found between the collection 4 and collection 5 Terra MODIS aerosol products (Remer et al., in press).

As mentioned in CHAPTER II, the observed reflectance at top of atmosphere (TOA) includes two parts: reflection by surface and atmosphere. For the surface reflectivity over ocean, three components are considered: (1) Fresnel reflection, (2) reflection scattered from objects located under the ocean surface like sediments, and (3) reflection from white foam, the coverage of which is a function of near surface wind speed (Koepke et al., 1979). A fixed near surface wind speed of  $6 \text{ m s}^{-1}$  is assumed in current retrievals (Remer et al., 2005). Uncertainties associated with this assumption will be discussed in later chapters. Additionally, no aerosol retrieval is performed over glint regions with glint angle less than  $35^\circ$ , where the water surface appears intensely bright due to specular reflection. The glint angle is defined as the angular difference between real reflection and mirror reflection.

Using predetermined atmospheric conditions, surface conditions, viewing geometries, and aerosol models, a LUT of simulated satellite radiances was generated as function of aerosol properties that include aerosol effective radius, single scattering albedo, asymmetry factor, phase function and  $\tau$ . Single scattering albedo is defined as the ratio of the aerosol scattering to the aerosol extinction. Asymmetry factor and phase function represent the angular distribution of aerosol scattering. The calculated aerosol radiance is the summation of reflected radiances from both small mode and large mode aerosols with a weight parameter of  $\eta$  (explained in CHAPTER II). The retrieval process

is then performed by matching the observed and LUT radiances and selecting the aerosol models and aerosol optical properties associated with output that minimizes

$$\varepsilon = \sqrt{\frac{\sum_{\lambda=1}^6 N_{\lambda} \left( \frac{\rho_{\lambda}^m - \rho_{\lambda}^{LUT}}{\rho_{\lambda}^m + 0.01} \right)^2}{\sum_{\lambda=1}^6 N_{\lambda}}} \quad (4.1)$$

where  $\varepsilon$  is error parameter,  $\lambda$  is wavelength,  $\rho_{\lambda}^m$  and  $\rho_{\lambda}^{LUT}$  are the observed and calculated radiance at wavelength  $\lambda$ , respectively, and  $N_{\lambda}$  is the sum of valid pixels at wavelength  $\lambda$  (Remer et al., 2005). A control value of  $\varepsilon < 3\%$  is used. If more than one solution falls within this range, an average of these qualifying solutions is used. If no solution falls within this range, an average of the best three solutions is used.

In addition to  $\tau$  and  $\eta$ , the MODIS aerosol products also contain other variables, such as observation conditions, aerosol microphysical properties, and a quality control (QC) flag, which may be derived from other bands. The QC flag separates confident retrievals from “bad” retrievals such as retrievals that could be contaminated by thin cirrus clouds (Levy et al., 2003; Tanré et al., 1997). Negative  $\tau$  values are included in the MODIS Collection 5 aerosol products and are caused by inherent radiometric uncertainties (Hyer et al., in press). However, these negative  $\tau$  values can easily be removed by using a quality control flag.

#### MISR and Algorithm

The Multi-angle Imaging SpectroRadiometer (MISR) is also on board the TERRA satellite. In contrast to MODIS, MISR has nine different viewing angles at nadir,  $\pm 26.1$ ,  $\pm 45.6$ ,  $\pm 60.0$ , and  $\pm 70.5$  degrees. Simultaneously, MISR has 4 spectral bands at 446.4

nm, 557.5 nm, 671.7 nm, and 866.4 nm. MISR also has a swath of 360 km, which is much narrower than MODIS's swath.

Additional information from the nine viewing angles can be used to study aerosol scattering at different angles. This enables the use of MISR data to estimate aerosol particle shape and size, and possibly aerosol absorption. Thus, addition to  $\tau$ , the MISR aerosol products also include more information, such as aerosol composition and size, surface directional reflectance factors, and bi-hemispherical reflectance.

Over dark oceans, the basic retrieval strategy for MISR is based on a similar LUT method that was described in the previous section. But instead of generating standard aerosol models, the MISR aerosol retrieving scheme categorizes aerosols as sea spray, sulfate/nitrate, mineral dust, biogenic particles and urban soot (Diner et al., 1998). The physical and chemical properties of these categorized aerosols are already known and prescribed. The mixing of these predetermined aerosol types is accomplished using a modified linear mixing theory (Martonchik et al., 1998).

A comparison of two years of MISR and AERONET data performed by Kahn et al. (2005) showed that two thirds of MISR AOD ( $\tau$ ) products values have an uncertainty of  $\pm 0.05$  or  $0.2 \times \tau_{AERONET}$ , wherein  $\tau_{AERONET}$  is the corresponding AERONET AOD value.

#### AERONET and Algorithm

AERONET (*A*Erosol *R*Obotic *N*ETwork) is a worldwide network and consists of more than 200 sun photometers which provide observations of aerosols by directly measuring the spectral extinction of sunlight. Derived from eight spectral bands from 0.34  $\mu\text{m}$  - 1.64  $\mu\text{m}$ , AERONET data (Holben et al., 1998) provide a long-term, continuous measurement of aerosol optical, microphysical and radiative properties.

AERONET data are considered as ground truth for validating model simulations and satellite retrievals.

The sun photometer operates at two different modes, one for direct sun measurements and another for sky measurements (Holben et al., 1998). The direct sun measurements are for measuring the direct and the diffuse radiation, from which aerosol optical depth values are computed using the Beer-Bouguer's Law after considering the influence of Rayleigh scattering and gas absorption (Holben et al., 1998). Sky measurements involve two basic observation sequences, the "almucantar plane" and the "principal plane", and are used to retrieve aerosol microphysical properties such as size distribution and phase function. Sky measurements involve series of measurements of radiances from aureole and sky through a series of scattering angles from the sun. The almucantar plane scan measures sky radiances at different azimuth angles relative to the sun at the elevation angle of the sun. The standard principal plane scan measures sky radiances at different scattering angles away from the sun in the principle plane (Holben et al., 1998).

Three AERONET data sets are available: level 1.0, 1.5, and 2.0. The level 1.0 AERONET data are raw data, the level 1.5 are cloud screened data, and the level 2.0 data are a subset of the level 1.5 data that have been quality assured (Smirnov et al., 2000). Eck et al. (1999) illustrated that the level 2.0 AERONET  $\tau$  are more accurate with an uncertainty ranging from 0.01 to 0.02, although these values may be slightly higher in the UV spectra. Both the AERONET level 1.5 and 2.0 data are used in this study. While level 2.0 data are used in most of these discussions, level 1.5 data are used to validate the MISR aerosol products, because the data volume of the MISR aerosol products are much

smaller than that of MODIS. As a consequence, after collocating MISR with the AERONET level 2.0 data, there are not enough pairs of data for statistical analysis.

A comparison of collocated AERONET level 1.5 data and level 2.0 data (collocation methods are explained in CHAPTER V) is shown in Fig.4. Although some outliers exist, there is no significant difference between these two AERONET products (Fig. 4).

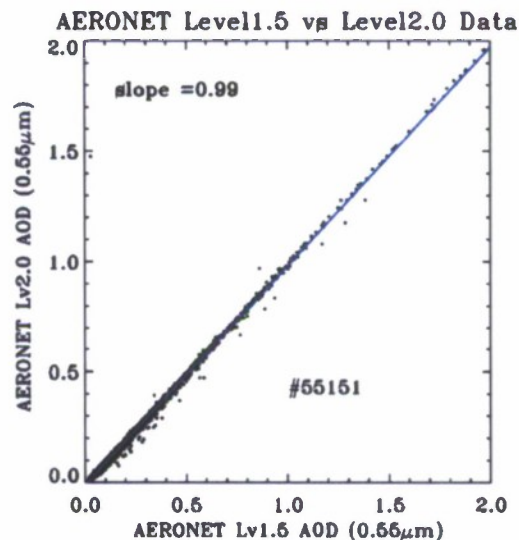


Figure 4. Scatter plots of the level 1.5 versus level 2.0 AERONET  $\tau$  at  $0.55 \mu\text{m}$  for 2005. Blue line is a linear regression line for all data.

#### NOGAPS Wind Speed Data

Near surface wind speed data from the Navy Operational Global Analysis and Prediction System (NOGAPS) weather forecast model (Hogan and Rosmond, 1991) were collected to investigate the effect of wind speed on MISR and MODIS aerosol retrievals. NOGAPS wind speed data (with assimilation of satellite observed wind speed data) are available four times a day at a spatial resolution of  $1^\circ$  latitude and longitude (Zhang and Reid, 2006).

CHAPTER V  
UNCERTAINTY ANALYSIS

Collocation Methods

In order to evaluate satellite aerosol products, satellite and ground-based observations have to be matched. Thus, as the first step, both MODIS and MISR satellite aerosol products were collocated with ground-based AERONET data. To minimize the spatial and temporal difference between these data, pairs of AERONET sun photometer data and MODIS/MISR aerosol retrievals were matched if the spatial distance between two observations was within  $0.3^\circ$  (latitude/longitude) and the difference in observation times was within 30 minutes.

AERONET data that are within  $\pm 30$  minutes of satellite overpasses were averaged. However, the satellite observations are not averaged spatially. The averaging process of surface observations reduces the sample biases, but could also filter out real signal peaks. For example, if a small scale smoke plume passes through a sun-photometer site, the averaged AERONET  $\tau$  value could be lower than the  $\tau$  value retrieved via a satellite. Also, it is possible that one AERONET observation could be paired with more than one satellite retrievals.

Many studies, different from this study, used averaged satellite and sun photometer data to blur the spatial and temporal differences between the two data sets (Remer et al., 2005; Kahn et al., in press; Hsu et al., 2006). This approach is understandable considering the spatial and temporal differences between the observations.

Sun photometer provides point observations at a given time whereas a satellite retrieval is a two dimensional spatial observation at a given time. Because of the difference in sampling methods, differences between the two types of observations can exist. However, in this study, in order to study the uncertainties in the satellite retrievals due to observing conditions at the pixel level, satellite data were not averaged. Note that only over ocean retrievals were used, which implies that only AERONET data from coastal or island sites were selected.

Four collocated data sets are included in this study. (1) MODIS Collection 5 aerosol products and AERONET level 1.5 data from 2005 to 2007; (2) MODIS Collection 5 aerosol products and the AERONET level 2.0 data from the year 2005; (3) MISR Version 22 aerosol products and AERONET level 1.5 data from 2005 to 2006; (4) MODIS, MISR and AERONET level 1.5 data from the year 2005. Because cloud information is not included in the MISR aerosol products, the fourth data set is used to provide MODIS cloud masks for MISR data analysis. Note that most of the subsequent discussions use only the Terra MODIS products. Similar results were obtained using the Aqua MODIS aerosol retrievals.

AERONET and satellite data are collocated at three wavelengths:  $0.55 \mu\text{m}$  for MODIS and  $0.558 \mu\text{m}$  for MISR,  $0.67$  and  $0.87 \mu\text{m}$ . Note that the AERONET data do not include observations at  $\lambda=0.55 \mu\text{m}$  and, therefore, the AERONET observations from  $0.50$  and  $0.67 \mu\text{m}$  were used to interpolate and match MODIS results at  $\lambda=0.55 \mu\text{m}$ . This interpolation is based on the assumption that the Angström Exponent ( $\alpha$ —further discussed in the *microphysical properties* section) derived from two wavelengths is consistent throughout all wavelengths (O'Neill, et al., 2001), with the relationship

$$\tau_{550} = \exp \left\{ \ln(\tau_{500}) + \left[ \frac{\ln\left(\frac{550}{500}\right)}{\ln\left(\frac{670}{500}\right)} \right] \times \ln\left(\frac{\tau_{670}}{\tau_{500}}\right) \right\} \quad (5.1)$$

where  $\tau_{550}$ ,  $\tau_{500}$  and  $\tau_{670}$  are  $\tau$  at 0.55  $\mu\text{m}$ , 0.5  $\mu\text{m}$  and 0.67  $\mu\text{m}$  bands, respectively.

To study the effect of near surface wind speed on satellite aerosol retrievals, NOGAPS wind data were also collocated to match all four of the data sets discussed above. Because the NOGAPS wind data are only available at four fixed times per day (00:00, 06:00, 12:00, and 18:00 UTC), aerosol data are coupled with the wind data by matching the observation time with the closest model output time. Notice that the time difference between the MODIS and the NOGAPS data could introduce bias to this study and will be evaluated in future studies.

#### Sources of Uncertainties

Three major sources of uncertainties can affect the accuracy of satellite derived aerosol properties. They are lower boundary conditions, cloud contamination and cloud artifacts, and uncertainties in the predetermined aerosol microphysical properties. Uncertainties caused by these three factors are discussed in the following sections.

#### *Lower Boundary Condition*

As described in the MODIS retrieval algorithm, ocean surface brightness, a key parameter in satellite aerosol retrievals, is strongly affected by near surface wind speed, especially for glint and near-glint regions and for regions, with white foams. Currently, a fixed near surface wind speed of 6  $\text{m s}^{-1}$  (Remer, et al., 2005) is used in the MODIS aerosol retrieval scheme. An increase in surface reflection can be contributed by two sources: an increase in the area of white foam coverage and variations in glint patterns,

both of which can be mistakenly attributed to aerosol contributed reflectance and thus can introduce a high bias to the retrieved  $\tau$  values. The impacts of these two sources on MISR aerosol products are much smaller, because multi-angle measurements from MISR can provide additional information to identify the background brightness information (Kahn, et al., 2005a).

To evaluate the impact of near surface wind speed on satellite aerosol retrievals, differences between AERONET and satellite  $\tau$  ( $\Delta\tau$ ) were examined as a function of NOGAPS wind speed (from 0 m s<sup>-1</sup> to 14 m s<sup>-1</sup>) for all three wavelengths. Figure 5a shows the AOD difference between level 2.0 AERONET and Terra MODIS Collection 5 ( $\Delta\tau_{A2.0\_MODTER}$ ). The  $\Delta\tau_{A2.0\_MODTER}$  values were averaged for every 2m s<sup>-1</sup> of wind speed. To minimize possible cloud contamination, satellite retrievals with reported cloud fraction larger than 80% were not used in this analysis. As Fig.5a demonstrates,  $\Delta\tau_{A2.0\_MODTER}$  at  $\lambda=0.55$   $\mu\text{m}$  monotonically decreases from -0.01 to -0.08 as the near surface wind speed increases from 0 to 14 m s<sup>-1</sup>. Similar patterns are also presented for the  $\Delta\tau_{A2.0\_MODTER}$  at  $\lambda=0.67$  and 0.87  $\mu\text{m}$ . Thus, an actual wind speed of 6 m s<sup>-1</sup> leads to a positive bias of 0.02 in MODIS retrieved  $\tau$  at  $\lambda=0.55$   $\mu\text{m}$ . When actual wind speed is smaller than 6 m s<sup>-1</sup>, a less overestimation of  $\tau$  are expected and vice versa. This finding is very similar to that of Zhang and Reid (2006) for the collection 4 MODIS aerosol products, indicating that the bias due to the wind speed still exists for the collection 5 MODIS aerosol products.

Wind effects were also studied using three years of collocated data for AERONET level 1.5 data and the Terra MODIS aerosol products as shown in Fig. 5b. The differences between the two aerosol products ( $\Delta\tau_{A1.5\_MODTER}$ ) are shown as a function of

wind speed. Similar but linear relationships were found in this study due to a larger data sample pool. The  $\Delta\tau_{A1.5\_MODTER}$  reaches -0.06 at a wind speed of  $14 \text{ m s}^{-1}$ , which is less than the  $\Delta\tau_{A2.0\_MODTER}$  value under same condition. All three wavelengths show similar results.

No significant biases in the MISR aerosol products were found when studied relative to near surface wind speed. The multi-angle measurements of MISR allow adjustment for wind speed effects while the MODIS single mode results in difficulties (Diner et al., 1998). MISR can always have cameras observing at large glint angles (non-glint region) when one or two angles fall into small glint angles (glint regions), and therefore, glint effects can be minimized.

#### *Cloud Contamination and Cloud Artifacts*

Cloud contamination and cloud artifacts have been well known problems in satellite aerosol studies (Zhang and Reid, 2006). Sub-pixel size clouds and/or thin cirrus clouds may not be detectable by the cloud screening methods during the aerosol retrieval process and, thereby, can introduce a high bias to satellite-retrieved  $\tau$  values. For example, Zhang and Reid (2006) found that MODIS  $\tau$  values increase with increasing cloud fraction and concluded that 75% of this increase was due to cloud contamination or cloud artifacts. Debates are ongoing regarding the causes of higher  $\tau$  values observed in the vicinity of clouds. Researchers have suggested that this bias could result from three-dimensional cloud effects (Wen, et al., 2006) or evaporation of cloud droplets (Koren, et al., 2007). Additionally, thick aerosol plumes could be misidentified as clouds (Obrecht 2008) and therefore be removed from the aerosol retrieval process, which causes a low

bias to satellite-derived  $\tau$  values. In either case, the impacts of clouds on satellite aerosol products need to be studied.

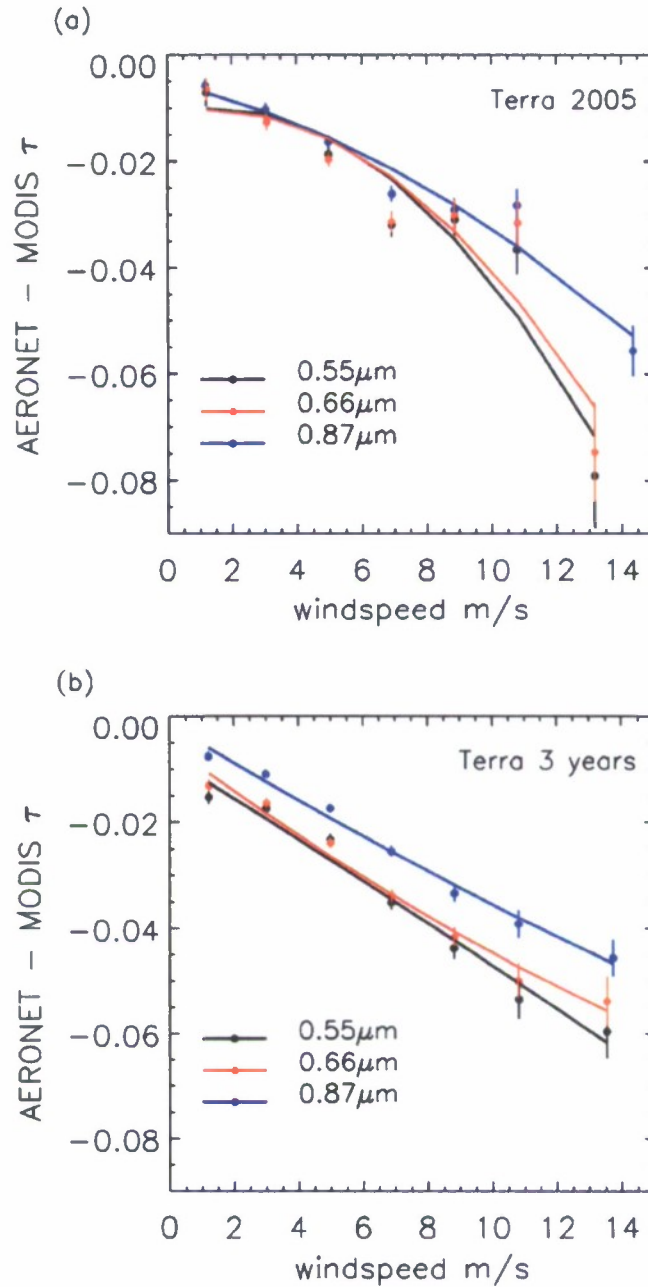


Figure 5. AERONET minus Terra MODIS  $\tau$  versus NOGAPS near-surface wind speed (a) using AERONET level 2.0 data for the year 2005. (b) using AERONET level 1.5 data and for the year 2005-2007.

Figure 6 shows scatter plots of AERONET level 2.0  $\tau$  (y axis) versus Terra MODIS  $\tau$  (x axis) at 0.87  $\mu\text{m}$  for six MODIS cloud fraction ranges: 0%, 0-20%, 20-40%, 40-60%, 60-80%, and 80-100%. Both AERONET and Terra MODIS  $\tau$  values at the 0.87  $\mu\text{m}$  were used for isolating the bias related to cloud amount from other satellite retrieving uncertainties. Note that channels with lower wavelengths such as 0.55  $\mu\text{m}$  are also strongly influenced by aerosol microphysical effects (discussed in *Microphysical Properties*). Not surprisingly, as the cloud fractions increase from 0 to 80-100%, the slopes of the linear regression line decrease from 0.96 to 0.85, indicating that cloud contamination and cloud artifacts introduce a high bias to the MODIS-retrieved  $\tau$  values. Furthermore, given these results this high bias could be categorized as a function of cloud fraction and removed from the data set. Figure 7 shows comparisons of AERONET level 1.5 data versus the Terra MODIS during a 3 years period, and demonstrates similar results to Fig. 6, which confirms that the results shown in Fig. 6 are rather robust.

Figure 8 is again similar to Fig. 6, but for the comparisons between AERONET level 1.5 and MISR  $\tau$  data. MODIS cloud mask data were used here to report the percentage of cloud cover within a MISR pixel. The overlap of cloud fraction from 50% to 80% in the last two cloud fraction categories shown in Fig. 8c and 8d was used to avoid having an insufficient data sample under high cloud conditions. Figure 8 shows that with increased cloud fractions, the slopes of the linear regression line of  $\tau$  decrease from 1.12 to 0.85. These similar results indicate that clouds also influence MISR-based  $\tau$  retrievals. However, to correct for these effects, the MISR cloud mask is required.

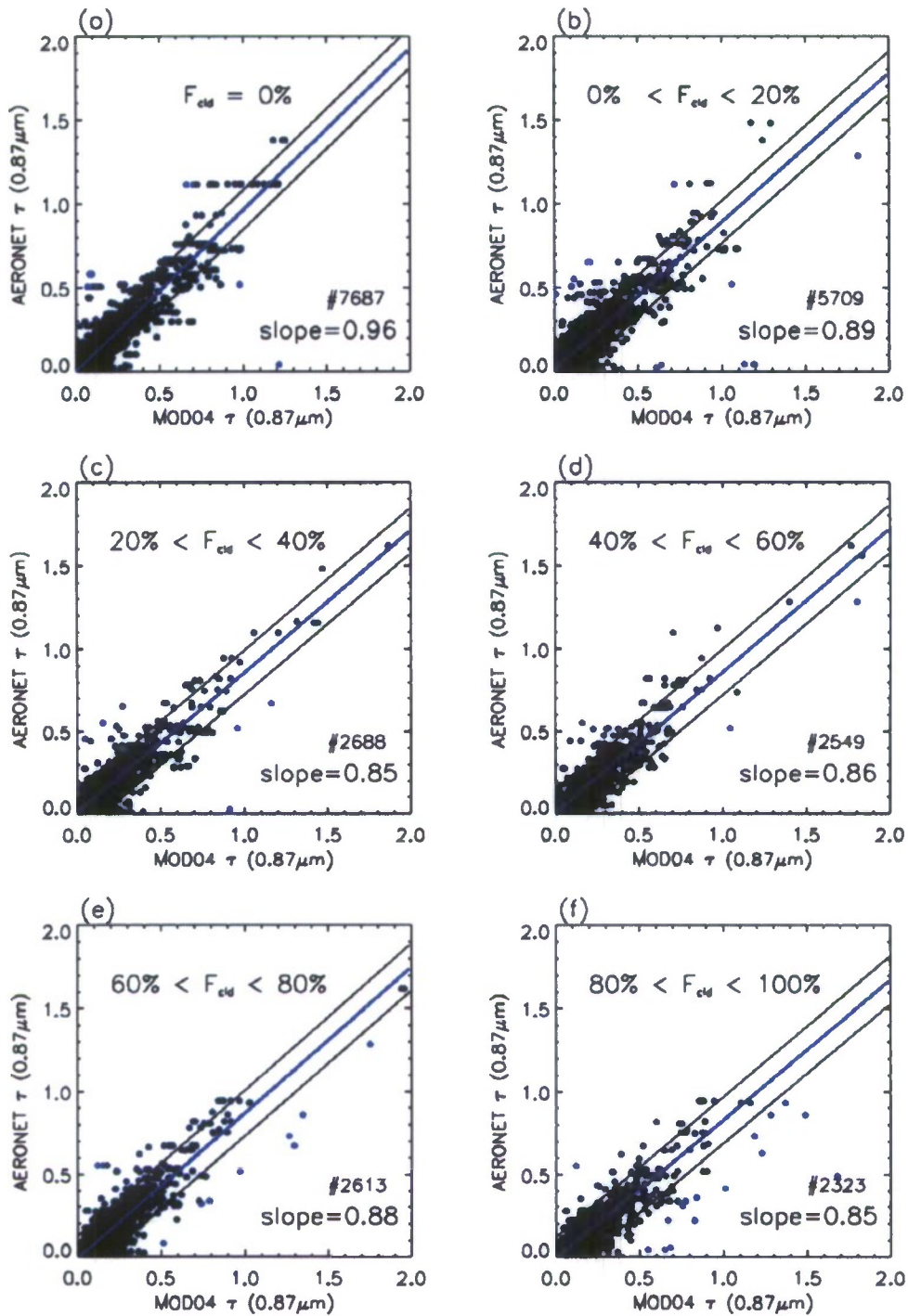


Figure 6. MODIS Terra versus AERONET level 2.0  $\tau_{0.87}$  as function of cloud fraction for the year 2005 for cloud fractions  $F_{cld}$  of (a) 0%, (b) 0-20%, (c) 20-40%, (d) 40-60%, (e) 60-80%, and (f) 80-100%. Blue lines are linear regression lines through the data points and the black lines show the 95% confidence interval of the blue lines. Blue dots are considered to be outliers that have an absolute difference between MODIS and AERONET  $\tau$  larger than 0.4.

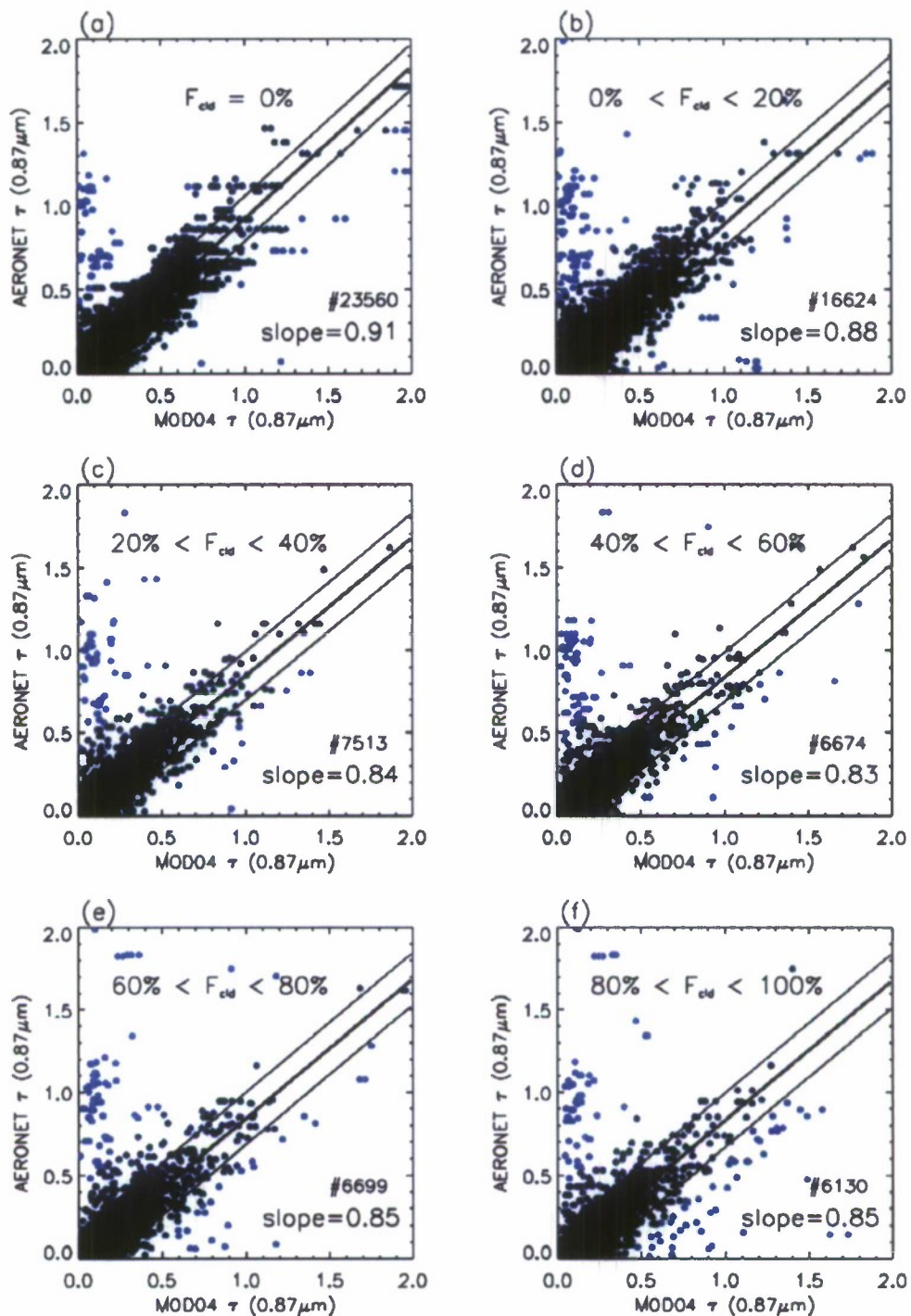


Figure 7. Terra MODIS versus AERONET level 1.5  $\tau_{0.87}$  as a function of cloud fraction for the year 2005-2007 for cloud fractions  $F_{\text{cld}}$  of (a) 0%, (b) 0-20%, (c) 20-40%, (d) 40-60%, (e) 60-80%, and (f) 80-100%. Blue lines are linear regression lines through the data points and the black lines show the 95% confidence interval of the blue lines. Blue dots are considered to be outliers that have an absolute difference between MODIS and AERONET  $\tau$  larger than 0.4.

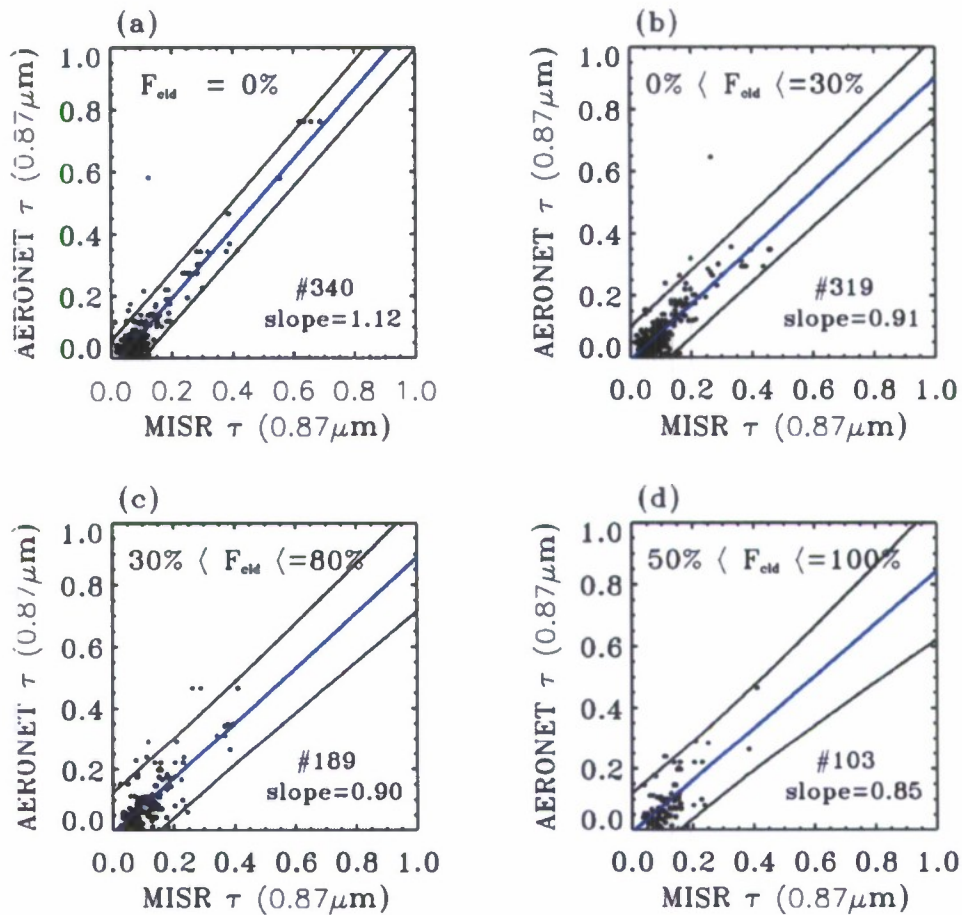


Figure 8. MISR versus AERONET level 1.5  $\tau_{0.87}$  as a function of cloud fraction for the year 2005 and 2006 for cloud fractions  $F_{cloud}$  of (a) 0%, (b) 0-30%, (c) 30-80%, and (d) 50-100%. Blue lines are linear regression lines through the data points and the black lines show the 95% confidence interval of the blue lines. Blue dots are considered to be outliers that have an absolute difference between MISR and AERONET  $\tau$  larger than 0.4.

### *Microphysical Properties*

In satellite aerosol retrieval algorithms, some aerosol physical and optical parameters such as the single-scattering albedo and the asymmetry factor are predetermined. However, parameters, such as the optical depth, are retrieved from LUT and the inversion process. Several sensitivity studies have shown that the predefined constant parameters used in these models have a significant influence on aerosol retrievals (Zhang and Reid, 2006). For example, Ichoku et al. (2005) found an

underestimation of MODIS  $\tau$  values over South Africa and concluded that this underestimation could be due to inaccuracies in aerosol models used in the retrieval process. Thus, it is necessary to evaluate satellite aerosol retrieved  $\tau$  against aerosol microphysical properties such as  $\eta$ .  $\eta$  is well studied and is included in the MODIS aerosol products, which makes the future empirical corrections and bias removal feasible. Therefore,  $\eta$  can be used as a parameter to investigate the impact of aerosol microphysics uncertainties on the retrieved  $\tau$  values, as shown in Fig 9.

Figure 9 shows the comparison between MODIS derived  $\tau$  and AERONET  $\tau$  as a function of the sun photometer retrieved  $\eta$  ( $\eta_{sp}$ ), where the fine mode  $\tau$  values with corresponding  $\eta_{sp}$  values larger than 0.7 are typically underestimated (Fig. 9a), while for coarse mode with corresponding  $\eta_{sp}$  values less than 0.45 are generally overestimated (Fig. 9b). Figure 9d confirms that an overestimation of  $\tau$  occurs when coarse particles dominate, indicating the necessity of removing this microphysical-based aerosol bias. This finding is consistent with what was reported by Zhang and Reid (2006).

Note that the MODIS-reported  $\eta$  values are the end result of the retrieval process. The Terra MODIS  $\eta$  values were evaluated against the AERONET derived  $\eta$ , as shown in Fig. 10. AERONET  $\eta$  were calculated using  $\tau$  values at four or more wavelengths based on O'Neil's algorithm (2001). Figure 10 shows a comparison between the Terra MODIS  $\eta$  and the AERONET-derived  $\eta$ . Even though large differences exist between MODIS  $\eta$  and AERONET  $\eta$ , their correlation is 0.50, indicating that it is possible to use MODIS  $\eta$  as a proxy for aerosol microphysics.

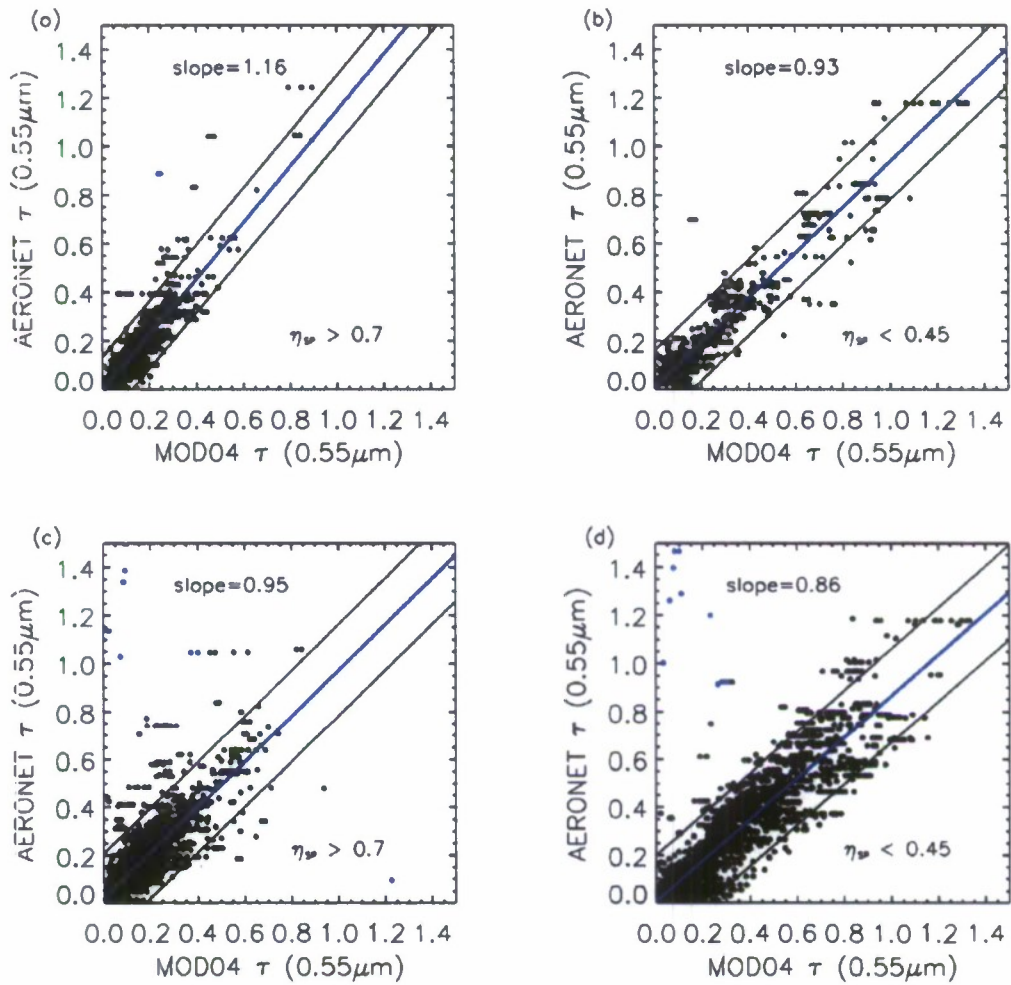


Figure 9. Terra MODIS versus AERONET  $\tau_{0.55}$  for two ranges of  $\eta$  based on AERONET  $\eta_{sp}$ . (a) & (b) using AERONET level 2.0  $\tau_{0.55}$  for year 2005. Blue lines are linear regression lines through the data points and the black lines show the 95% confidence interval of the blue lines. Blue dots are considered as outliers that have absolute difference between MODIS and AERONET  $\tau$  larger than 0.6. (c) & (d) As in (a) & (b) respectively, but with for AERONET level 1.5  $\tau$  data for 2005-2007.

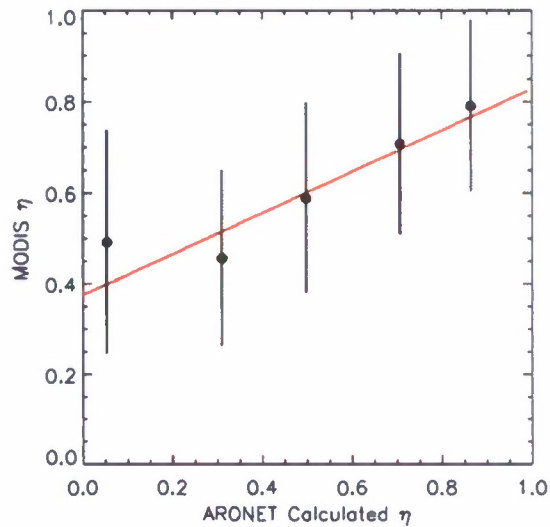


Figure 10. Scatter plot of the MODIS fine mode fraction and AERONET-derived fine mode fraction at the 0.55  $\mu\text{m}$  wavelength. The black dots are averaged MODIS  $\eta$  for every 0.2 of AERONET  $\eta$  with one standard deviation, red line is a linear regression line for all the  $\eta$  points.

Because the biases and uncertainties in  $\tau$  can be a function of both cloud fraction and the MODIS reported  $\eta$ , Fig. 11 and Fig. 12 demonstrates the slopes of MODIS and AERONET  $\tau$  as functions of both cloud fraction and  $\eta$  using AERONET level 2.0 and level 1.5, respectively. Figure 11a shows that at 0.55  $\mu\text{m}$  the slopes are mostly larger than 1 for small particles ( $\eta > 0.7$ ) and smaller than 0.95 for coarse particles ( $\eta < 0.45$ ), while at 0.87  $\mu\text{m}$  (Fig. 11c) slopes are almost independent of  $\eta$ . Therefore, aerosol microphysical effects appear to be more important for shorter wavelengths. Also, in all three figures (Fig. 11a-c) the slopes decrease with increased cloud fraction for both fine mode and coarse mode aerosols, showing that cloud contaminations and cloud artifacts impact retrievals at all three wavelengths and need to be corrected. Similar patterns are found in Fig. 12. These results indicate that empirical corrections to MODIS  $\tau$  values are possible when cloud fraction and  $\eta$  effects are considered simultaneously.

The Angström Exponent was used to evaluate the aerosol microphysical effects on the MISR aerosol products, because  $\eta$  is not included in its products. The Angström Exponent ( $\alpha$ ) is expressed as

$$\alpha = -\ln\left(\frac{\tau_{\lambda_1}}{\tau_{\lambda_2}}\right) / \ln\left(\frac{\lambda_1}{\lambda_2}\right) \quad (5.2)$$

where  $\tau_{\lambda_1}$  and  $\tau_{\lambda_2}$  are the aerosol optical depth values at wavelengths  $\lambda_1$  and  $\lambda_2$ . Similar to  $\eta$ , large  $\alpha$  values indicate predominance of small sized particles and small  $\alpha$  values indicate predominance of large sized particles. Figure 13a shows the absolute  $\tau$  difference ( $\Delta\tau$ ) between AERONET level 1.5 and MISR as a function of the Angström Exponent for each of the three wavelengths: 0.55  $\mu\text{m}$  (black), 0.66  $\mu\text{m}$  (red), and 0.87  $\mu\text{m}$  (blue). As shown in Fig. 13a large biases around 0.035 exist for large particles when  $\alpha$  is smaller than 0.7 at all three wavelengths. The  $\Delta\tau$  at  $\lambda=0.55$   $\mu\text{m}$  band is systematically greater than 0.025, while for the 0.87  $\mu\text{m}$  band it increases from -0.04 to 0 with the increasing Angström Exponent. This indicates that aerosol microphysics have a large effect on the MISR aerosol products. This large bias in the 0.55  $\mu\text{m}$  band may be caused by calibration issues. To further evaluate the microphysical effects that are found with the 0.55  $\mu\text{m}$  band,  $\Delta\tau$  for the 0.55  $\mu\text{m}$  band was analyzed as a function of the Angström Exponent for low ( $0.0 < \tau < 0.2$ ), middle ( $0.2 < \tau < 0.4$ ), and high ( $0.4 < \tau < 2.0$ )  $\tau$  conditions (Fig. 13b). In both low and middle aerosol loading cases,  $\Delta\tau$  values are consistently around -0.025 regardless of the Angström Exponent. In the high aerosol loading case,  $\Delta\tau$  increases from -0.08 to 0 as the Angström Exponent increases from 0.0

to 1.5. Figure 13b indicates that  $\tau$ -dependent corrections need to be applied to ameliorate aerosol microphysical effects on the MISR aerosol products for each  $\tau$  case.

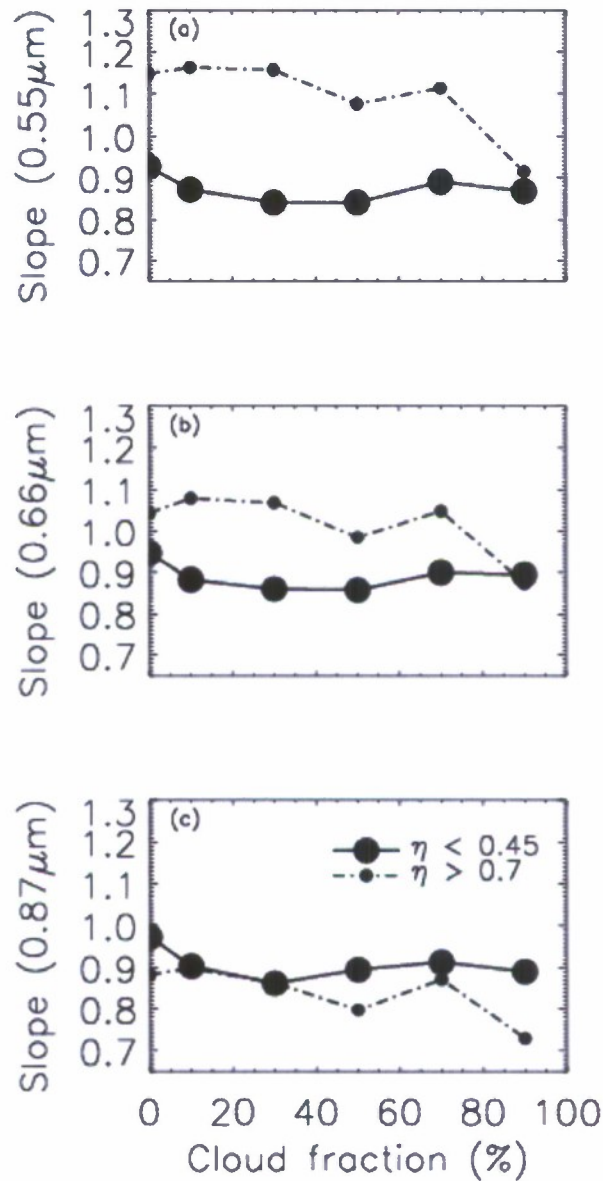


Figure 11. Slope of MODIS versus AERONET level 2.0  $\tau$  (as shown in Fig 9a and 9b) as function of cloud fraction and two fine mode fraction from AERONET for the year 2005. Cloud Fraction range: 0%, 0-20%, 20-40%, 40-60% 60-80%, and 80-100%. Solid line represents  $\eta$  less than 0.45 and dashed line represents  $\eta$  greater than 0.7. (a) For 0.55  $\mu\text{m}$ . (b) For 0.66  $\mu\text{m}$ . (c) For 0.87  $\mu\text{m}$ .

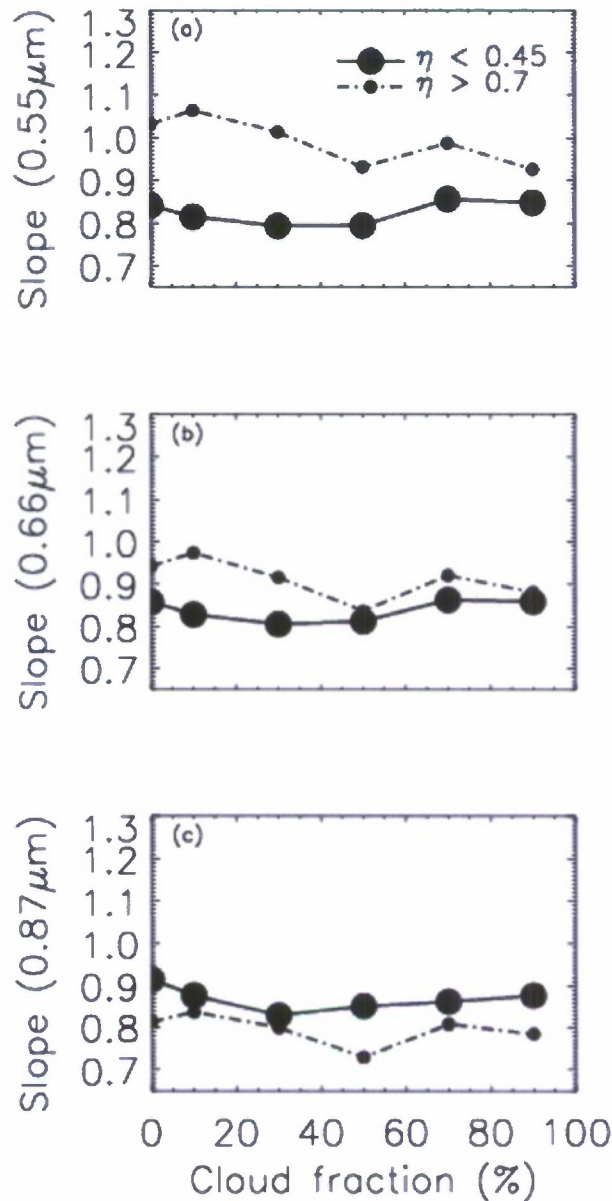


Figure 12. Slope of MODIS versus AERONET level 1.5  $\tau$  (as shown in Fig 9c and 9d) as function of cloud fraction and two fine mode fraction from AERONET for the year 2005-2007. Cloud Fraction range: 0%, 0-20%, 20-40%, 40-60%, 60-80%, and 80-100%. Solid line represents  $\eta$  less than 0.45 and dashed line represents  $\eta$  greater than 0.7. (a) For 0.55  $\mu\text{m}$ . (b) For 0.66  $\mu\text{m}$ . (c) For 0.87  $\mu\text{m}$ .

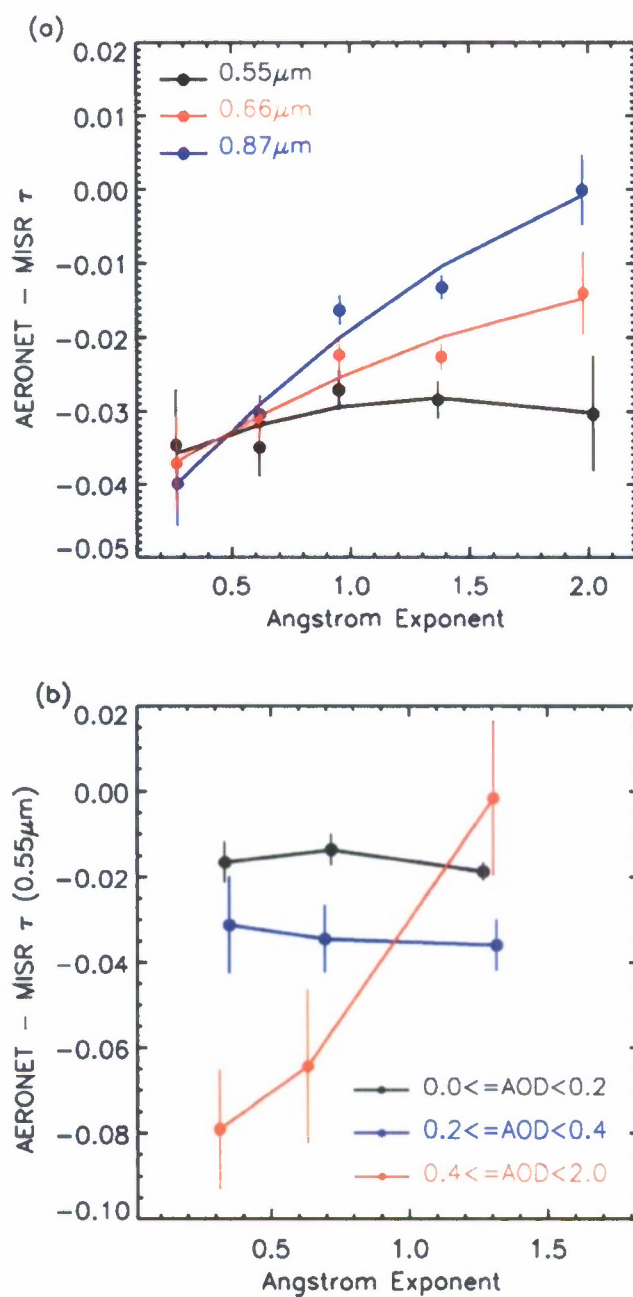


Figure 13. Microphysical effects on MISR aerosol products. (a) The differences in the AERONET level 2.0 and the MISR  $\tau$  ( $\Delta\tau$ ) versus aerosol Angström Exponent for year 2005 and 2006, and for three wavelengths, 0.55 (black), 0.67 (red) and 0.87  $\mu\text{m}$  (blue). The dots present the averaged  $\Delta\tau$  for the different Angström Exponent ranges (0-0.4, 0.4-0.8, 0.8-1.1, 1.1-1.8, and 1.8-3.4). (b) The differences in the AERONET level 2.0 and the MISR  $\tau_{0.55}$  ( $\Delta\tau_{0.55}$ ) versus the aerosol Angström Exponent with  $\tau$  ranges 0-0.2, 0.2-0.4, and 0.4-2.0. The dots present the averaged  $\Delta\tau_{0.55}$  for the different Angström Exponent ranges (0-0.5, 0.5-0.9, and 0.9-3.6).

CHAPTER VI  
RESULTS AND DISCUSSIONS

As illustrated in the previous chapter, biases and uncertainties in the satellite reported  $\tau$  values are functions of observing conditions, and can be studied and systematically removed or reduced. In this chapter (as shown in Fig. 14), empirical correction and quality assurance (QA) procedures are developed, evaluated and applied, and new versions of level 3 MODIS and MISR aerosol products are generated.

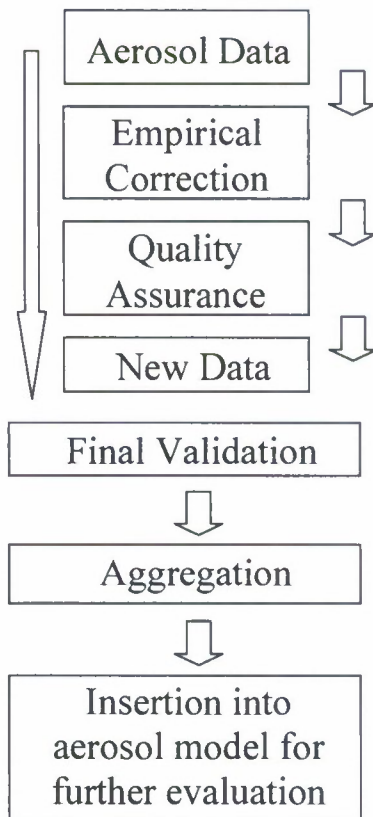


Figure 14. Data Processes Flow Chart.

## Empirical Corrections

According to the uncertainty analyses described in the previous chapter, developing empirical corrections that could automatically diminish the cloud artifacts, surface wind speed effects, and aerosol microphysics effects, is possible and important. The procedures for developing empirical equations for the MODIS and MISR aerosol optical depth products at the 0.55  $\mu\text{m}$  band spectrum will be described separately.

The MODIS empirical corrections were developed in two steps: (1) low  $\tau$  case ( $\tau_{550} < 0.2$ ), where biases in the aerosol products are highly dependent on the lower boundary conditions, such as the near surface wind speed and cloud artifacts; (2) high  $\tau$  case ( $\tau_{550} > 0.2$ ), where aerosol microphysical effects and cloud contamination are critical. The empirical correction equations were derived using collocated AERONET versus MODIS data for both Terra and Aqua.

For the low MODIS  $\tau$  case, data with MODIS  $\tau_{550}$  less than 0.2 were categorized in three ranges of glint angle ( $30^\circ$ - $60^\circ$ ,  $60^\circ$ - $80^\circ$ , and  $80^\circ$ - $260^\circ$ ). The glint angle was calculated using

$$\psi_{glint} = \cos^{-1}[(\cos\theta_s \cos\theta_v) + (\sin\theta_s \sin\theta_v \cos\phi)] \quad (6.1)$$

where  $\theta_s$ ,  $\theta_v$ , and  $\phi$  are the solar zenith, satellite viewing zenith, and the difference between sun and satellite azimuth angles, respectively (Levy et al., 2003). Regression lines were then created using the NOGAPS near surface wind speed ( $u$ ) and the MODIS cloud fraction ( $F_{cld}$ ) for each of the glint angle ranges:

$$\tau_{new} = \tau_{old} + A - B \times u - C \times F_{cld} \quad (6.2)$$

where A, B, and C are coefficients that vary with glint angle and the values of which are shown in Table 1. Table 1 shows that for small glint angles ( $\psi < 60^\circ$ ), the corrections are larger, and as the glint angle increases, biases caused by wind are largely reduced.

Table 1. Coefficients for Terra and Aqua as A Function of Glint Angle ( $\psi$ ) for (6.2).

			A	B	C
TERRA	MODIS vs. AERONET 2.0 (2005)	$30^\circ < \psi < 60^\circ$	0.0267	0.0047	0.00039
		$60^\circ < \psi < 80^\circ$	0.0164	0.0031	0.00039
		$\psi > 80^\circ$	0.0099	0.0018	0.00001
	MODIS vs. AERONET 1.5 (2005-2006)	$30^\circ < \psi < 60^\circ$	0.0287	0.0043	0.00029
		$60^\circ < \psi < 80^\circ$	0.0145	0.0025	0.00030
		$\psi > 80^\circ$	0.0116	0.0014	0.00029
AQUA	MODIS vs. AERONET 2.0 (2005)	$30^\circ < \psi < 60^\circ$	0.0288	0.0051	0.00033
		$60^\circ < \psi < 80^\circ$	0.0212	0.0033	0.00031
		$\psi > 80^\circ$	0.0150	0.0012	0.00040
	MODIS vs. AERONET 1.5 (2005-2006)	$30^\circ < \psi < 60^\circ$	0.0352	0.0052	0.00027
		$60^\circ < \psi < 80^\circ$	0.0219	0.0023	0.00025
		$\psi > 80^\circ$	0.0155	0.0012	0.00029

For the high MODIS  $\tau$  cases ( $\tau_{550} > 0.2$ ), a multivariate analysis was applied using the MODIS  $F_{cld}$  and  $\eta$ . Wind speed effects were not included because the uncertainties due to boundary conditions are of less significance in high aerosol loading cases.

Although  $\eta$  values derived from AERONET were used to analyze microphysical effects,  $\eta$  values from the MODIS aerosol products were implemented in the application of the correction procedures. This is because AERONET data cannot provide sufficient spatial coverage for correcting the MODIS aerosol products. Based on the evaluation of MODIS  $\eta$  in the preceding uncertainty analysis, it is reasonable to use  $\eta$  from MODIS to perform correction.  $\eta$  was only applied in high  $\tau$  cases. This is because large uncertainties exist when retrieving  $\eta$  in low  $\tau$  cases, where aerosol signals are weak (Kleidman et al., 2005).

The empirical equation for this step is

$$\tau_{new} = \tau_{old} \times (D - E \times F_{cld} + F \times \eta) + G \quad (6.3)$$

with the values of the coefficients  $D$ ,  $E$ ,  $F$ , and  $G$  provided in Table 2. Table 2 indicates that cloud fraction and  $\eta$  are of critical importance. For example, a 100% change in cloud fraction and  $\eta$  could lead to a 20% and 40-50% change in MODIS  $\tau_{550}$ , respectively.

Table 2. Coefficients for (6.3).

		$D$	$E$	$F$	$G$
TERRA	MODIS vs. AERONET 2.0 (2005)	0.778	0.0022	0.431	0.00026
	MODIS vs. AERONET 1.5 (2005-2006)	0.820	0.0016	0.259	0.00564
AQUA	MODIS vs. AERONET 2.0 (2005)	0.734	0.0016	0.536	-0.00186
	MODIS vs. AERONET 1.5 (2005-2006)	0.791	0.0021	0.420	0.00636

For the MISR  $\tau_{558}$  products, only the microphysical correction was applied to the empirical correction. Because no significant relationship between the surface wind speed and the MISR  $\tau$  was found. Furthermore, although cloud effects exist in its aerosol retrievals, cloud mask data for MISR, which were not available in this study, are required for applying the cloud corrections. As a result, the empirical correction equation for MISR is only a function of the Angström Exponent for high  $\tau$  cases. In low  $\tau$  cases ( $\tau_{558} < 0.4$ ), as shown in Fig. 13b, MISR  $\tau$  values are systematically higher than AERONET  $\tau$  by approximately 0.02. Thus, to adjust  $\tau_{558}$  smaller than 0.4, an offset of -0.02 was applied, regardless of the Angström Exponent. For high  $\tau$  cases ( $\tau_{558} > 0.4$ ),  $\Delta\tau$  changes significantly with the Angström Exponent ( $\alpha$ ) and the empirical equation for this case is:

$$\tau_{new} = (0.825 + 0.0979 \times \alpha) \times \tau_{old} + 0.008 \quad (6.4)$$

This shows that before and after correction, the slope of  $\tau$  can change as much as 10% with a 100% change of the Angström Exponent value.

#### Quality Assurance Analysis

Quality assurance steps are performed after the empirical corrections to ensure that cloud contaminated pixels and isolated retrievals are removed from the final products. The three separate steps for this procedure are: standard error check, buddy check, and QA flag check.

A standard error check was performed to determine the spatial variation of the  $\tau$  values around a valid retrieval. Pixels with high spatial variations of  $\tau$  were removed. This technique was used to detect retrievals near the edges of the clouds, as studies have found a correlation between MODIS  $\tau_{550}$  and cloud fraction (Loeb and Manalo-Smith, 2005) that can be attributed mostly to cloud contamination and cloud artifacts (Zhang et al., 2005a). Standard error is calculated using:

$$STD\_error = \frac{\sigma}{\sqrt{N}} \quad (6.5)$$

where

$$\sigma = \sqrt{\frac{1}{N} \sum_{i=1}^N (x_i - \mu)^2} \quad (6.6)$$

$N$  is the sample size,  $x_i$  is the  $i^{\text{th}}$  sample value,  $\mu$  is the expected value, and  $\sigma$  is standard deviation. Here standard error was calculated for every 3 x 3 pixels around a given point.

Figure 15a and 15b shows the standard error as function of MODIS and MISR  $\tau$ , respectively. The 1.5 standard deviation lines serve as an upper limit. Data above this line are considered to have an unacceptable standard error. The relations

$$STD\_error = 0.003 + 0.050 \times \tau_{0.55} + 0.024 \times \tau_{0.55}^2 \quad (6.7)$$

$$STD\_error = 0.002 + 0.047 \times \tau_{0.55} - 0.001 \times \tau_{0.55}^2 \quad (6.8)$$

represent this limit for MODIS and MISR  $\tau$  respectively. All data samples that have calculated standard error larger than these thresholds have been removed in the following results. An evaluation of the essentiality of this step will be presented later.

Buddy checks were then performed to remove isolated pixels. A given pixels is removed if there are no valid retrievals among its immediate neighbors, which indicates this pixel could be located between clouds.

The quality flag included in the aerosol products is utilized as a last step to filter the data. Only retrievals that are flagged as “best” and “good” data, with reported cloud fraction less than 80%, were used.

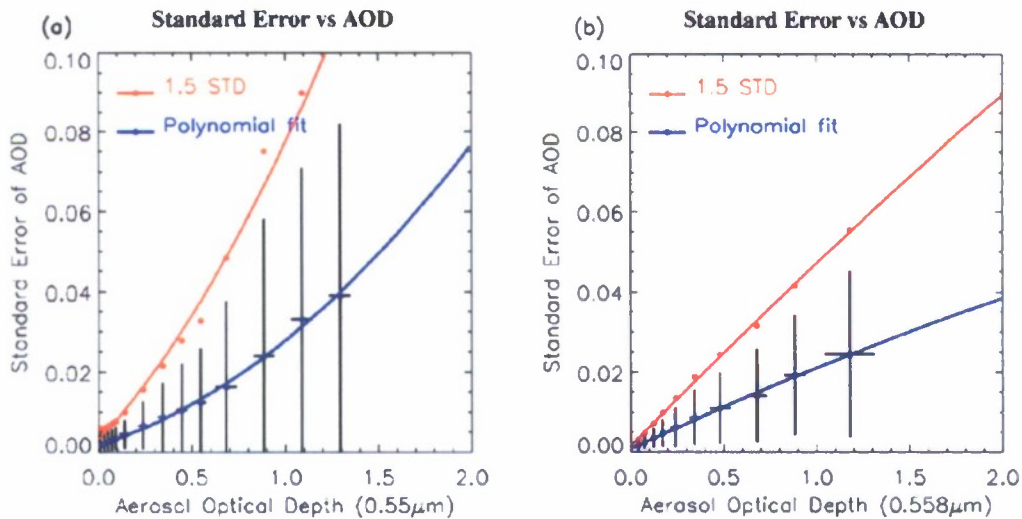


Figure 15. Scatter plot of standard error of  $\tau$  versus  $\tau$ . Dots represent the averaged Standard Error (blue) of  $\tau$  and 1.5 standard deviation (red) for every 0.05 of  $\tau$  when  $\tau < 0.5$  and 0.3 of  $\tau$  when  $\tau > 0.5$ . The blue and red lines show the second order polynomial fitting of corresponding dots. (a) For MODIS  $\tau_{550}$ . (b) MISR  $\tau_{558}$ .

#### Validation

Using empirical corrections and quality assurance procedures developed in the previous section, new  $\tau$  data sets from the MODIS Terra Collection 5 over ocean and MISR Version 22 aerosol products were generated for 2005.

To evaluate the newly developed  $\tau$  data sets, inter-comparisons were made using the  $\tau$  values from the new data sets against the AERONET level 2.0 data for 2005 as shown in Fig. 16 and Fig. 17. Figure 16a shows a comparison of AERONET level 2.0 and the original MODIS Collection 5  $\tau$  and Fig. 16b shows a comparison of AERONET level 2.0  $\tau$  and the newly generated MODIS  $\tau$  using empirical equations generated from the MODIS and AERONET level 2.0 for 2005. Comparing Fig. 16a and b, the original slope of the MODIS versus AERONET  $\tau$  is corrected and most outliers (as indicated by red circles) are removed. One important parameter for evaluating the quality of the new data set is the absolute  $\tau$  difference between MODIS and AERONET, where the absolute difference between MODIS and AERONET  $\tau$  decreases by 20% from 0.052 to 0.042 and by 10% from 0.083 to 0.073 in high  $\tau$  cases ( $\tau_{\text{AERONET}} > 0.2$ ). The slope of the linear fit line (blue line) increases from 0.79 to 1.02. The standard deviations of data in low and high  $\tau$  cases decrease by 0.01. A 1.5 standard deviation of standard error threshold and an 80% of cloud fraction threshold were chosen for these results with a data loss of 34.1%.

Figure 18a and b show a comparison of the MISR and AERONET level 1.5 values before and after corrections for 2005. The absolute difference between the MISR and AERONET  $\tau$  generally decreases by 10%, which is from 0.045 to 0.040 for all data and from 0.067 to 0.058 for high  $\tau$  cases. The slopes of the linear fit line increases from 0.90 to 0.99. Correlation between the MISR and AERONET data increases from 0.91 to 0.93 with several outliers were removed. The same thresholds were chosen as 80% of cloud fraction and 1.5 standard deviation of standard error, with a data loss of 56.7%.

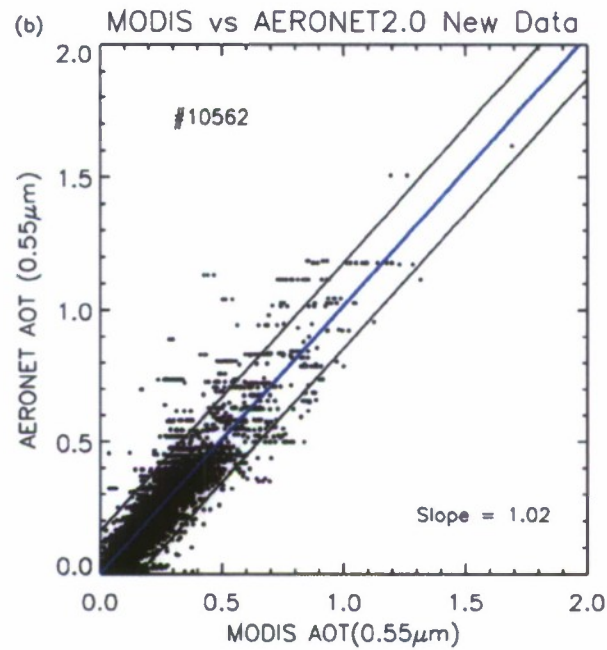
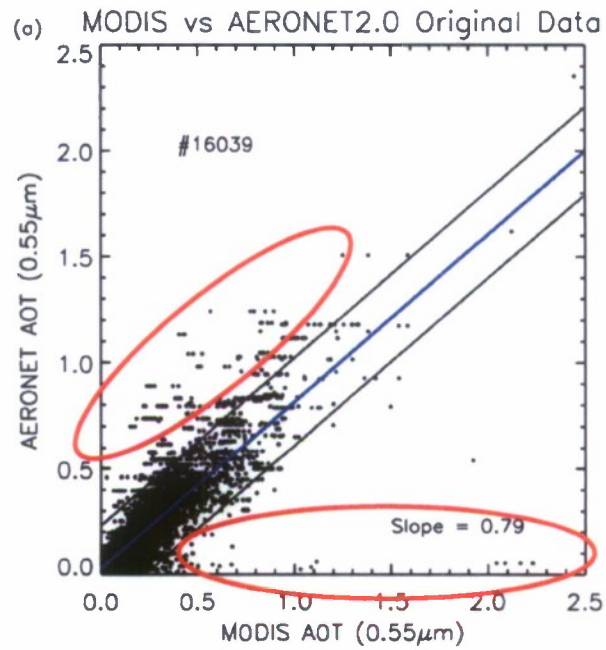


Figure 16. Scatter plot of Terra MODIS versus AERONET level 2.0  $\tau_{550}$  for 2005. The blue line is the linear regression line for all data and black lines are 95% confidence interval of blue line. (a) With Terra MODIS Collection 5. (b) With newly generated Terra MODIS  $\tau_{550}$ .

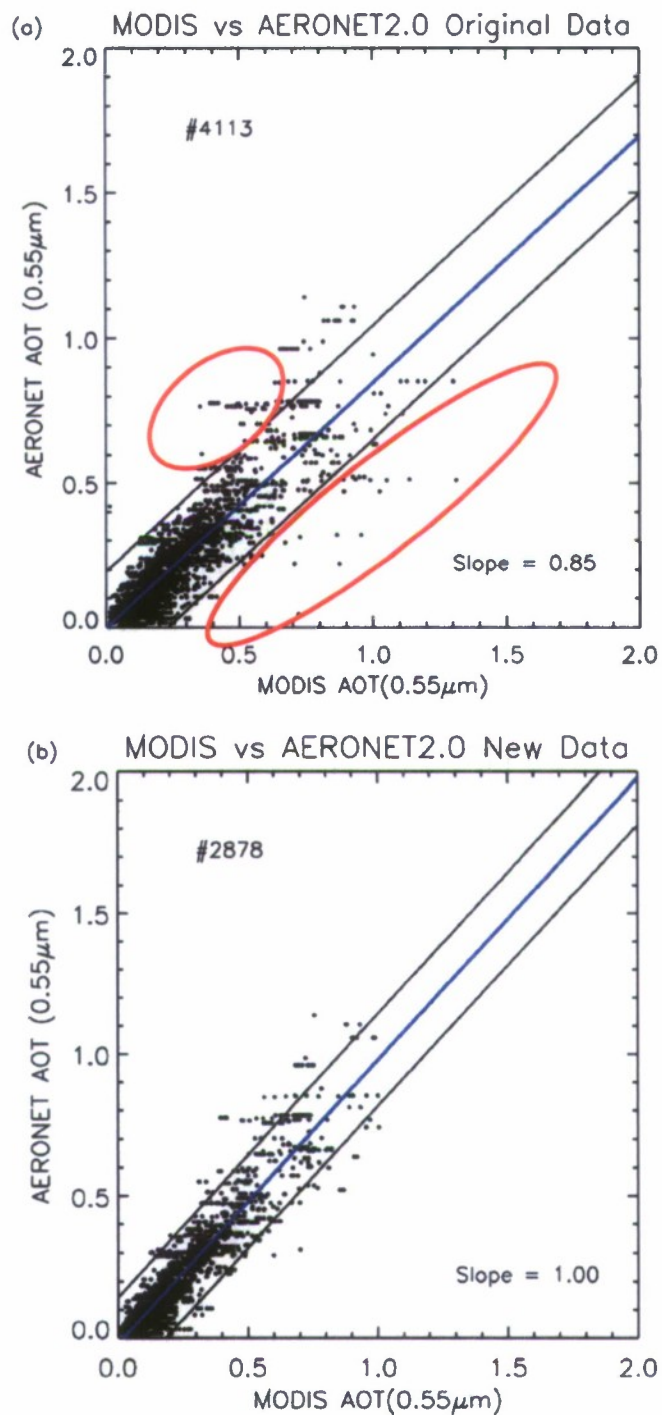


Figure 17. Scatter plot of Terra MODIS versus AERONET level 2.0  $\tau_{550}$  for 2007. The blue line is the linear regression line for all data and black lines are 95% confidence interval of blue line. (a) With Terra MODIS Collection 5. (b) With newly generated Terra MODIS  $\tau_{550}$ .

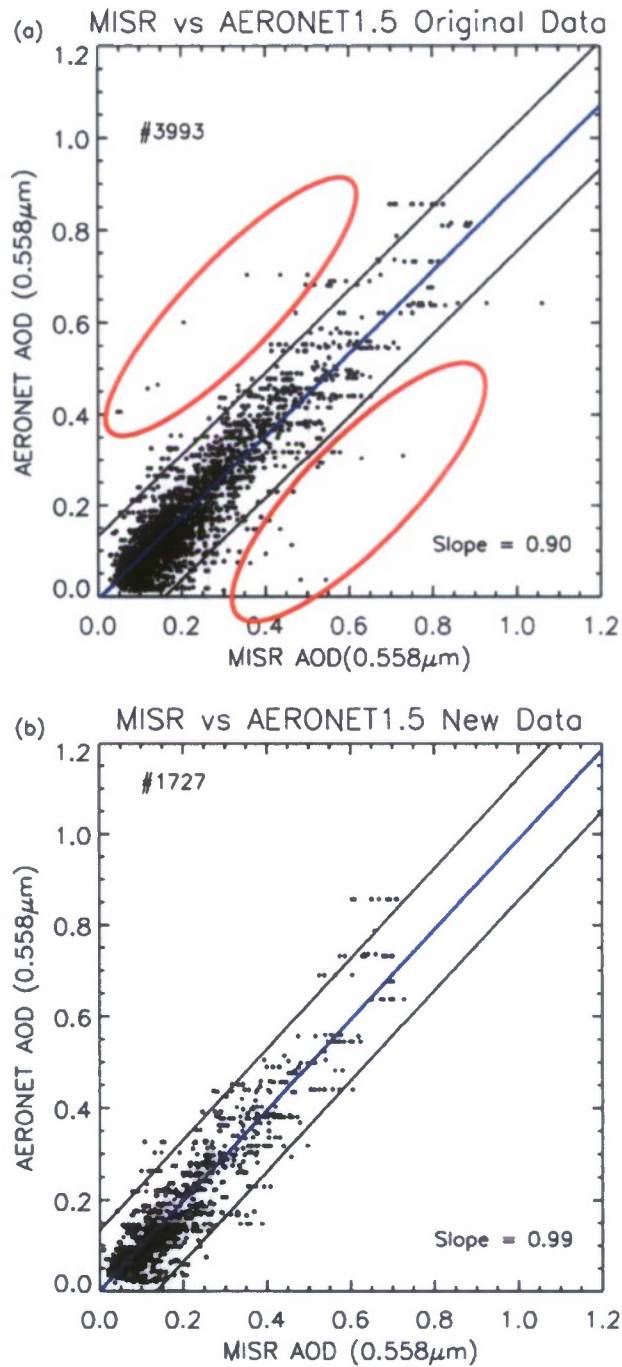


Figure 18. Scatter plot of the MISR versus the AERONET level 1.5  $\tau_{558}$  for 2005. The blue line is the linear regression line for all data and black lines are 95% confidence interval of blue line. (a) With MISR Version 22 products (b) With the newly generated MISR  $\tau_{558}$ .

## Independent Validation

The empirical corrections and quality assurance (QA) procedures were also validated through the study of independent data sets that are not used in generating (6.2) and (6.8). Figure 17a and b show the same comparisons as Fig. 16, except using the MODIS and AERONET level 2.0 data from January to May 2007. Figure 17a shows the scatter plot of the MODIS and AERONET  $\tau$  using the original MODIS Terra Collection 5 aerosol product. Figure 17b shows the similar plot as Fig. 17a, except the equations, which were applied to produce the new data were generated from the collocated MODIS and AERONET level 1.5 data for 2005 and 2006. Again, most noisy data points are removed and the original slope of the MODIS and AERONET  $\tau$  is improved from 0.85 to 1.0. The absolute  $\tau$  difference reduced by 17% from 0.061 to 0.050 for all data points, and 22% from 0.093 to 0.072 for high  $\tau$  cases. Figure 17 suggests that the empirical corrections and QA procedures developed in this study are robust.

## Spatial Evaluation

To demonstrate the changes for the newly generated data spatially, Fig. 19 was created by spatially averaging the  $\tau$  data in every one degree latitude and longitude square for 2005. Figure 19a and b show the spatial distributions of the original MODIS Terra Collection 5 and the newly developed data, respectively. The main features are similar before and after applying the empirical corrections and QA procedures, although the aerosol distribution patterns are smoother for the newly developed data set. This is because the standard error check step works as a high pass filter, which removes the high frequency noise while maintaining the low frequency signal. A huge reduction of  $\tau$  is found over the southern oceans (latitude from -40 to -60). A high  $\tau$  (0.3-0.5) zone is

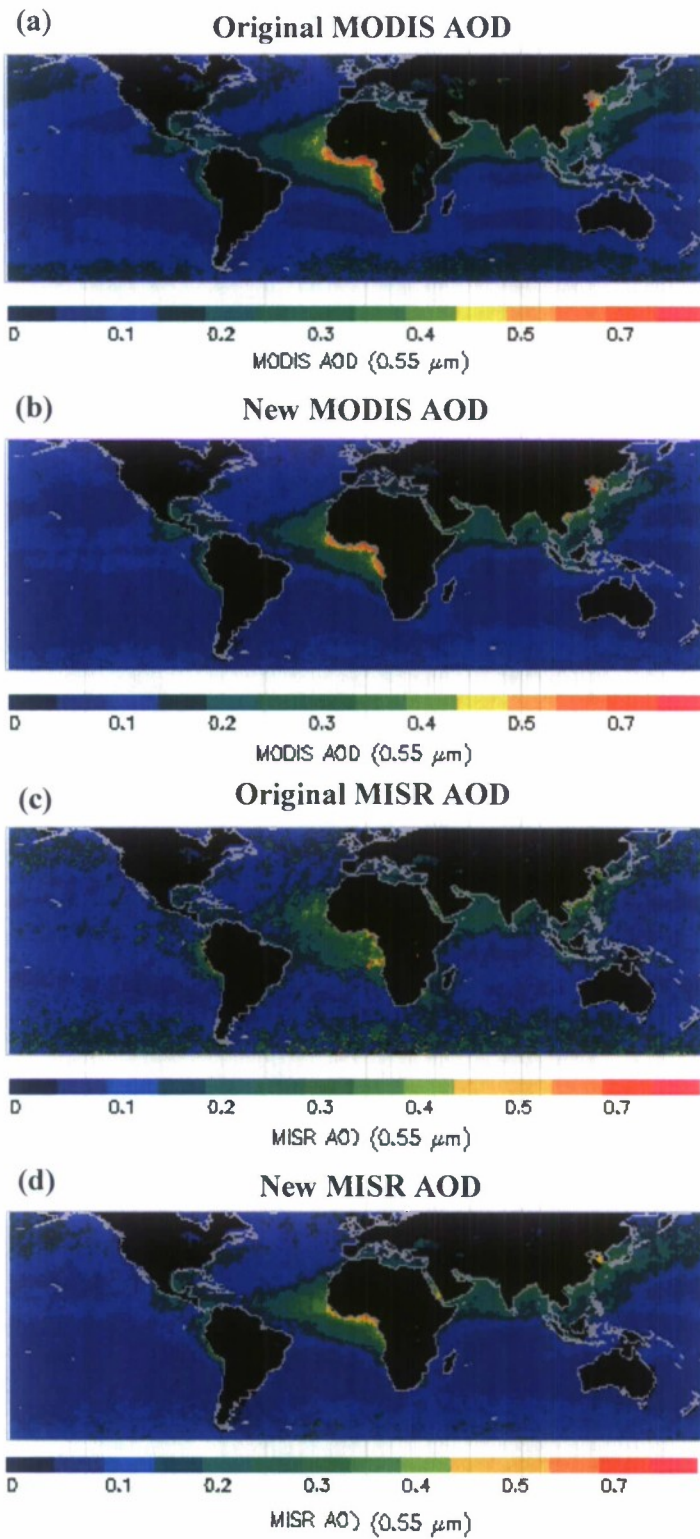


Figure 19. Spatial distribution of  $\tau$ . (a) With  $\tau_{550}$  from MODIS Collection 5. (b) As in (a) but for the newly generated MODIS  $\tau_{550}$ . (c) & (d) As in (a) & (b) but for MISR  $\tau_{558}$ .

located over the southern oceans in Fig. 19a, but this aerosol zone is not found in Fig. 19b, indicating that this high  $\tau$  zone might be caused by cloud contamination and thus was mostly removed by standard error check step. Figure 19c and d show the plots similar to those in Fig. 19a and b, but for the MISR aerosol products before and after applying empirical corrections and QA procedures. Again, the primary patterns are preserved and the suspiciously high  $\tau$  band over the southern oceans is removed, suggesting that the potential cloud contamination issue exists in the MISR aerosol products as well.

### Sensitivity Study

Thresholds such as the cloud fraction cutoff are included in the quality assurance procedures. Table 3 shows the statistics before and after application of corrections to the MODIS Terra and AERONET level 2.0 aerosol data. As shown in Table 3, the quality assurance step is the procedure that removes a large portion of data. The question arises as to whether a threshold can be chosen to optimize the data quality while minimizing the data loss. A sensitivity study was performed to determine suitable thresholds using the same collection of data as shown in Table 3. Table 3 shows the slopes, correlations, and absolute errors of comparisons between the MODIS (after correction) and AERONET  $\tau$  as functions of thresholds used in the corrections (such as cloud fraction, standard error cutoff, and quality flag). It showed that generally a stricter cloud fraction cutoff of 50% causes an additional 10% of data loss and only a 2% of improvement in data quality when compared to an 80% of cloud fraction threshold. Therefore, a threshold of 80% cloud fraction was selected and all data with an 80% cloud fraction or higher was removed. A threshold of 1.0 standard deviation of standard error (STD of SE) is not ideal because it associates with a much larger data loss ratio yet with almost no increase in data quality

comparing with the use of the 1.5 STD of SE. Although statistical results from a threshold of 1.5 STD of SE is not greatly improved from that of 2.0, daily spatial distributions of  $\tau$  show that 1.5 STD of SE could remove certain noises caused by cloud contamination which is contained in 2.0 STD of SE. Thus, thresholds of 80% of cloud and 1.5 STD of SE were applied to generate new  $\tau$  products.

Table 3. Sensitivity studies of the empirical corrections and quality assurance procedures of Terra MODIS Collection 5 and the AERONET Level 2.0 Aerosol Products.

<i>Empirical Correction</i>	<i>n/a</i>	<i>applied</i>	<i>applied</i>	<i>applied</i>	<i>applied</i>	<i>applied</i>	<i>applied</i>	<i>applied</i>
<i>QA/QC</i>	<i>n/a</i>	<i>only cloud</i>	<i>applied</i>	<i>applied</i>	<i>applied</i>	<i>applied</i>	<i>applied</i>	<i>applied</i>
<i># STD of SE<sup>a</sup></i>	<i>n/a</i>	<i>n/a</i>	<i>1</i>	<i>1</i>	<i>1.5</i>	<i>1.5</i>	<i>2</i>	<i>2</i>
<i>Cloud Fraction</i>	<i>n/a</i>	<i>80%</i>	<i>80%</i>	<i>50%</i>	<i>80%</i>	<i>50%</i>	<i>80%</i>	<i>50%</i>
Absolute error <sup>b</sup>	0.0515	0.0468	0.0428	0.0416	0.0423	0.041	0.0437	0.0426
Absolute error <sup>c</sup>	0.0832	0.0772	0.0734	0.0709	0.0734	0.0709	0.0757	0.0737
Correlation	0.87	0.89	0.92	0.92	0.92	0.92	0.91	0.91
Slope	0.79	0.98	1.01	1.00	1.02	1.00	1.02	1.00
Data Loss Rate	0.0%	13.0%	34.6%	46.1%	34.1%	44.5%	23.5%	37.6%

<sup>a</sup>Number of standard deviation of standard error.

<sup>b</sup>Absolute error ( $\sum(|\Delta\tau_{0.55}|)/n$ ) for all data points.

<sup>c</sup>Absolute error for data points with MODIS  $\tau_{0.55} > 0.2$ .

## CHAPTER VII

### CONCLUSION AND FUTURE STUDY

This study evaluated uncertainties of satellite over water aerosol products by comparing satellite data with ground based AERONET data and by using three years of MODIS data and two years of MISR aerosol data. Uncertainties were examined as functions of near surface wind speed, cloud fraction, and aerosol microphysics in order to develop empirical correction procedures. Quality assurance steps were also established to remove data samples with possible cloud contamination. New products with less uncertainty were generated as level 3 over ocean MODIS and MISR aerosol products for future data assimilation and model use. The main conclusions of this study are:

- (1) Strong relationships were found between uncertainties in the MODIS Collection 5 aerosol products and three potential uncertainty sources: near surface wind speed, cloud fraction and microphysics, which is similar to what were shown in the MODIS Collection 4 aerosol products (Zhang and Reid, 2006).
- (2) No dependency between the MISR Version 22 aerosol products and the NOGAPS near surface wind speed was found. However, a relationship between the MISR  $\tau$  and the MODIS cloud fraction was identified. A systematic bias was found in the MISR aerosol optical depth as a function of the Angström Exponent.
- (3) This study suggests that after the QA and empirical corrections the quality of the over water operational MODIS (C5) and MISR aerosol products is improved by more than

17% for MODIS and 10% for MISR globally, and by more than 50% over the southern oceans according to reduction of  $\Delta \tau$ .

(4) The sensitivity study performed herein suggests that with 23% of data loss, the data quality increased by 15% for thresholds of 80% of cloud fraction and 2.0 STDs of SE. A threshold of 1.5 STDs of SE and 80% of cloud was chosen in order to reduce the bias caused by cloud effects and yet remain a sufficient amount of data.

As a future study, the MISR level 2.0 cloud products will be included into the analysis and an inter-comparison of the newly developed MODIS and MISR over water products will be made. The quality of the new data sets will also be evaluated through satellite data assimilation. Lastly, this study will be extended to a much longer period (2000-2008), and over land areas, by including products from other sources, such as the Deep Blue products (Hsu et al., 2006).

## REFERENCES

- Albrecht, B. A., (1989), Aerosols, Cloud Microphysics, and Fractional Cloudiness, *Science*, 15 September 1989 Vol. 245. no. 4923, pp. 1227-1230 DOI: 10.1126/science.245.4923.1227
- Andreae, M. O., C. D. Jones, and P. M. Cox, (2005), Strong Present-day Aerosol Cooling Implies a Hot Future, *Nature*, Vol 435|30 June 2005|DOI:10.1038/nature03671.
- Andreae, M. O., (2007), Aerosols before Pollution, *Science* Vol315. 10.1126|science. 1136529.
- Appel, B.R., Y. Tokiwa, J. Hsu, E.L. Kothny and E. Hahn, (1985), Visibility as Related to Atmospheric Aerosol Constituents, *Atmospheric Environment*, Volume 19, Issue 9, 1985, Pages 1525-1534, DOI:10.1016/0004-6981(85)90290-2.
- Bäurner, D., B. Vogel, S. Versick, R. Rinke, O. Mohler, M. Schnaiter, (2008), Relationship of Visibility, Aerosol Optical Thickness and Aerosol Size Distribution in An Ageing Air Mass over South-West Germany, *Atmospheric Environment* 42 (2008) 989-998.
- Bellouin, N., O. Boucher, J. Haywood, and M. S. Reddy, (2005), Global Estimate of Aerosol Direct Radiative Forcing from Satellite Measurements, *Nature* Vol 438|22/29 December 2005|DOI:10.1038/nature 04348.
- Brunekreef, B., G. Hoek, P. Fischer, and F. T. M. Spijksma, (2000), Relation between Airborne Pollen Concentrations and Daily Cardiovascular and Respiratory-Disease Mortality, *THE LANCET* | Vol 355 | April 29.
- Brock, C.A., H.H. Jonsson, J.C. Wilson, J.E. Dye, D. Baumgardner, S. Borrmann, M.C. Pitts, M.T. Osborn, R.J. DeCoursey, and D.C. Woods, (1993), Relationships between optical extinction, backscatter and aerosol surface and volume in the stratosphere following the eruption of Mt. Pinatubo, *Geophys. Res. Lett.*, 20, 2555--2558.
- Churg, A., and M. Brauer, (1997), Human Lung Parenchyma Retains PM2.5, *Am. J. Respir. Crit. Care Med.*, Vol 155, No. 6, Jun 1997, 2109-2111.
- Climate Change 2007 - The Physical Science Basis Contribution of Working Group I to the Fourth Assessment Report of the IPCC (ISBN 978 0521 88009-1 Hardback; 978 0521 70596-7 Paperback).

- Cooke, W.F., and J.J.N. Wilson, (1996), A Global Black Carbon Aerosol Model, *J. Geophys. Res.*, 101(D14), 19,395-19,409.
- Diner, D. J., J. C. Beckert, T. H. Reilly, C. J. Bruegge, J. E. Conel, R. A. Kahn, J. V. Martonchik, T. P. Ackerman, R. Davies, S. A. W. Gerstl, H. R. Gordon, J. Muller, R. B. Myneni, P. J. Sellers, B. Pinty, and M. M. Verstraete, (1998), Multi-angle Imaging SpectroRadiometer (MISR) Instrument Description and Experiment Overview, *IEEE Trans. Geosci. Remote Sens.*, VOL. 36, NO. 4, July 1998.
- Dzubay, T. G., R. K. Stevens, C. W. Lewis, D. H. Hern, W. J. Courtney, J. W. Tesch, and M. A. Mason, (1982), Visibility and aerosol composition in Houston, Texas, *Environ. Sci. Technol.*, 1982, 16 (8), pp 514-525 DOI: 10.1021/es00102a017.
- Eck, T. F., B. N. Holben, J. S. Reid, O. Dubovik, A. Smirnov, N. T. O'Neill, I. Slutsker, and S. Kinne, (1999), Wavelength Dependence of the Optical Depth of Biomass Burning, Urban, and Desert Dust Aerosols *J. Geophys. Res.* Vol 104, No. D24, Pages 31,333-31,349, December 27, 1999.
- Gunii, R. and B. B. Phillips, (1957), An Experimental Investigation of the Effect of Air Pollution on the Initiation of Rain, *J. Meteorol* 14, 272(1957) DOI: 10.1175/1520-0469(1957)014<0272:AEIOTE>2.0.CO;2.
- Hobbs, P. V. and L. F. Radke, (1969), Cloud Condensation Nuclei from a Simulated Forest Fire, *Science* 17 January 1969: Vol. 163. no. 3864, pp. 279 – 280 DOI: 10.1126/science.163.3864.279.
- Hogan, T. F., and T. E. Rosmond, (1991), The Description of the Navy Operational Global Atmospheric Prediction Systems Spectral Forecast Model, *Mon. Weather Rev.*, 119(8), 1786-1815, DOI:10.1175/1520-0493(1991)119<1786:TDOTNO>2.0.CO;2.
- Holben, B. N., T. F. Eck, I. Slutsker, D. Tanré, J. P. Buis, A. Setzer, E. Vermote, J. A. Reagan, Y. J. Kaufman, T. Nakajima, F. Lavenu, I. Jankowiak, and A. Smirnov, (1998), A ERONET-A Federated Instrument Network and Data Archive for Aerosol Characterization *Remote Sens. Environ.* 66:1-16 PII s003-4257(98)00031-5.
- Hsu, N. Christina, Si-Chee Tsay, Michael D. King, and Jay R. Herman, (2006), Deep Blue Retrievals of Asian Aerosol Properties During ACE-Asia. *IEEE transactions on geoscience and remote sensing* ISSN 0196-2892 CODEN IGRSD2. 2006, vol. 44 (1), no11, pp. 3180-3195.
- Hyer, E. J., J. Zhang and J. R. Reid, (in submitting), Filtering MODIS AOD to prepare for over-land aerosol data assimilation.

- Ichoku, C., L. A. Remer, and T. F. Eck, (2005), Quantitative Evaluation and Intercomparison of Morning and Afternoon MODIS Aerosol Measurements from Terra and Aqua Satellites J. Geophys. Res., 110,D10S03, DOI:10.1029/2004JD004987.
- Kahr, R. A., B. Gaitley, J. Martonchik, D. Diner, K. Crean, and B. Holben, (2005a), MISR Global Aerosol Optical Depth Validation based on Two Years of Coincident AERONET observations, J. Geophys. Res., DOI10:1029/2004JD004706.
- Kahr, R. A., D. L. Nelson, M. J. Garay, R. C. Levy, M. A. Bull, D.J. Diner, J. V. Martonchik, S. R. Paradise, E. G. Hansen and L. A. Remer (in press), MISR Aerosol Product Attributes and Statistical Comparisons with MODIS, Transactions on Geoscience and Remote Sensing. IEEE Trans. Geosci. Remote Sens.
- Kaufman, Y. J. and R. S. Fraser, (1997), The Effect of Smoke Particles on Clouds and Climate Forcing, Science 12 September 1997:Vol. 277. no. 5332, pp. 1636 – 1639 DOI: 10.1126/science.277.5332.1636.
- Kaufman, Y. J., D. Tauré, L. A. Remer, E. F. Vermote, A. Chu, and B. N. Holben, (1997a), Operational Remote Sensing of Tropospheric Aerosol Over Land from EOS Moderate Resolution Imaging Spectroradiometer, J. Geophys. Res., vol. 102, no. D14, pages17,051-17,067, July 27, 1997.
- Kaufman, Y. J., J. V. Martins, L. A. Remer, M. R. Schoeberl, and M. A. Yamasoe, (2002), Satellite Retrieval of Aerosol Absorption over the Oceans Using SunGlint, Geophys. Res. Lett., 29(19), 1928, DOI: 10.1029/2002GL015403, 2002.
- Kaufman, Y. J., D. Tanré, and O. Boucher, (2002), A Satellite View of Aerosols in the Climate System, Nature|VOL419| 12 September 2002|.
- Kaufman, Y. J., I. Koren, L. A. Remer, D. Rosenfeld, and Y. Rudich., (2005), The Effect of Smoke, Dust and Pollution Aerosol on Shallow Cloud Development over the Atlantic Ocean, PNAS August 9, 2005 | vol. 102 |no. 32 |11207.
- Kim, M., W. K. M. LAU, M. CHIN, K. KIM, Y. C. SUD, and G. K. WALKER, (2006), Atmospheric Teleconnection over Eurasia Induced by Aerosol Radiative Forcing during Boreal Spring, Journal of Climate, Vol 19, 4700-4718.
- Kleidman, R. G., N. T. O'Neil, L. A. Remer, Y. J. Kaufman, T. F. Eck, D. Tanré, O. Dubovik, and B. N. Holben, (2005), Comparison of MODIS and AERONET remote sensing retrievals of aerosol fine mode fraction over ocean, J. Geophys. Res., 110, D22205, DOI:10.1029/2005JD005760.

- Koepke, P., and H. Quenzel, (1979), Turbidity of the Atmosphere Determined from Satellite: Calculation of Optimum Viewing Geometry, *J. Geophys. Res.*, Volume 84, Issue C12, p. 7847-7856, DOI: 10.1029/JC084iC12p07847.
- Koren, I., Y. J. Kaufman, L. A. Remer, and J. V. Martins, (2004), Measurement of the Effect of Amazon Smoke on Inhibition of Cloud Formation, *Science* 27 February 2004:Vol. 303. no. 5662, pp. 1342 – 1345 DOI: 10.1126/science.1089424.
- Koren, I., L. A. Remer, Y. J. Kaufman, Y. Rudich, and J. Vanderlei Martins, (2007), On the twilight zone between clouds and aerosols, *Geophys. Res. Lett.*, 34, L08805, DOI: 10.1029/2007GL029253.
- Krewski, D., R. Burnett, M. Jerrett, C. A. Pope, D. Rainham, E. Calle, G. Thurston, and M. Thun, (2005), Mortality and Long-Term Exposure to Ambient Air Pollution: Ongoing Analyses Based on the American Cancer Society Cohort, *Journal of Toxicology and Environmental Health, Part A*, 68:13,1093-1109.
- Lau, K. M., M. K. Kim, and K. M. Kim (2006), Asian Summer Monsoon Anomalies Induced by Aerosol Direct Forcing: The Role of the Tibetan Plateau. *Climate Dynamics* (2006) 26: 855-864 DOI 10.1007/s00382-006-0114-z.
- Loeb, N.G., and Manalo-Smith, N (2005), Top-of-Atmosphere Direct Radiative Effect of Aerosols over Global Oceans from Merged CERES and MODIS Observations, *J. Climate*, 18, 3506-3526, 2005.
- Levy, R. C., L. A. Remer, D. Tanré, Y. J. Kaufman, C. Ichoku, B. N. Holben, J. M. Livingston, P. B. Russell, and H. Maring (2003), Evaluation of the Moderate-Resolution Imaging Spectroradiometer (MODIS) retrievals of dust aerosol over the ocean during PRIDE, *J. Geophys. Res.*, 108(D19), 8594, DOI: 10.1029/2002JD002460.
- Liu, L., and M. I. Mishchenko, (2008), Toward unified satellite climatology of aerosol properties: Direct comparisons of advanced level 2 aerosol products, *JQSRT* (2008), DOI:10.1016/j.jqsrt.2008.05.003.
- Martonchik, J. V., D. J. Diner, B. Pinty, M. M. Verstraete, R. B. Myneni, Y. Knyazikhin, and H. R. Gordon, (1998), Determination of Land and Ocean Reflective, Radiative and Biophysical Properties Using Multi-angle Imaging, *IEEE Trans. Geosci. Remote Sens.*, 36, 1266-1281, 1998.
- Nakajima, T., A. Higurashi, K. Kawamoto, and J. E. Penner, (2001), A Possible Correlation Between Satellite-Derived Cloud and Aerosol Microphysical Parameters. *Geophys. Res. Lett.* 28 1171-1174 2001.
- Obrecht, R. L. (2008), A Study of Asian Dust Events Using Surface, Satellite, and Aircraft Measurements During INTEX-B, Master thesis of UND 1-67.

- O'Dowd, C. D., M. H. Smith, I. E. Consterdine, and J. A. Lowe (1997), Marine Aerosol, Sea-salt, and The Marine Sulphur Cycle: A Short Review, *Atmospheric Environment*, Vol. 31, Iss. 1, January 1997, Pages 73-80, DOI:10.1016/S1352-2310(96)00106-9.
- O'Neill, N. T., O. Dubovik, T. F. Eck, (2001), A modified Angstrom Coefficient for The Characterization of Sub-micron Aerosols, *App. Opt.*, Vol. 40, No. 15, pp. 2368-2374, 2001.
- Peixoto, J. P. and A. H. Oort, (1992), *Physics of Climate*, Published by Springer, 1992 ISBN 0883187124, 9780883187128
- Ramanathan, V., P. J. Crutzen, J. T. Kiehl, and D. Rosenfeld, (2001), Aerosols, Climate, and the Hydrological Cycle, *Science* 7 December: Vol. 294. no. 5549, pp. 2119 – 2124 DOI: 10.1126/science.1064034.
- Remer, L. A., Y. J. Kaufman, D. Tanré, S. Mattoo, D. A. Chu, J. V. Martins, R.-R. Li, C. Ichoku, R. C. Levy, R. G. Kieidman, T. F. Eck, E. Vermote, and B. N. Holben, (2005), The MODIS Aerosol Algorithm, Products, and Validation, *Journal of Atmospheric Sciences*, vol. 62, Issue 4, pp.947-973 DOI: 10.1175/JAS3385.1.
- Remer, L. A., R. G. Kleidman, R. C. Levy, Y. J. Kaufman, D. Tanré, S. Mattoo, J. V. Martins, C. Ichoku, I. Koren, H. Yu, and B. N. Holben, (in press), Global Aerosol Climatology from The MODIS Satellite Sensors, *J. Geophys. Res.*
- Roberts, G., M. J. Wooster, and E. Lagoudakis, (2008), Annual and Diurnal African Biomass Burning Temporal Dynamics, *Biogeosciences Discuss.*, 5, 3623-3663.
- Squires, P., (1958), The Microstructure and Colloidal Stability of Warm Clouds, *Tellus*, 10,256 (1958).
- Tanré, D., Y.J. Kaufman, M. Herman, and S. Mattoo, (1997), Remote Sensing of Aerosol Properties Over Oceans Using the MODIS/EOS Spectral Radiances, *J. Geophys. Res.*, VOL 102, No.D14, Page 16,971-16,988, July 27. 1997.
- Tong, Y. P., G. L. Zhang, M. G. Tan, W. Wang, J. M. Chen, Y. Hwu, P. C. Fsu, J. H. Je., G. Margaritondo, W. M. Song, R. F. Jiang, and Z. H. Jiang, Synchrotron Microradiography Study on Acute Lung Injury of Mouse Caused by PM2.5 Aerosols, LSE-ARTICLE-2006-003 LPRX-ARTICLE-2006-003

- Venkataraman, C., G. Habib, A. Eiguren-Fernandez, A. H. Miguel, and S. K. Friedlander, (2005), Residential Biofuels in South Asia: Carbonaceous Aerosol Emissions and Climate Impacts, *Science* 307, 1454 (2005); DOI: 10.1126/science.1104359.
- Wang, J. and S. A. Christopher, (2003), Intercomparison between Satellite-derived Aerosol Optical Thickness and PM<sub>2.5</sub> Mass: Implications for Air Quality Studies. *Geophys. Res.*, Vol 30, No. 21, 2095, DOI: 10.1029/2003GL018174, 2003.
- Wen, G., A. Marshak, and R. F. Cahalan, (2006), Impact of 3-D Clouds on Clear-Sky Reflectance and Aerosol Retrieval in a Biomass Burning Region of Brazil, *IEEE Trans. Geosci. Remote Sens.*, Vol. 3, No. 1, January 2006.
- Whitby, K.T., (1978), The Physical Characteristics of Sulfur Aerosols, *Atmos. Environ.*, vol 12, Issues 1-3, pp. 135-159, 1978.
- Zhang, J., J. S. Reid, and B. N. Holben, (2005a), An analysis of potential cloud artifacts in MODIS over ocean aerosol optical thickness products, *Geophys. Res. Lett.*, 32, L15803, DOI:10.1029/2005GL023254.
- Zhang, J., and J. S. Reid, (2006), MODIS Aerosol Product Analysis for Data Assimilation: Assessment of Over-Ocean level 2 Aerosol Optical Thickness Retrievals, *J. Geophys. Res.*, Vol.111. D22207, DOI: 10.1029/2005JD006898.
- Zhang, J., and J. S. Reid, (2008), A System for Operational Aerosol Optical Depth Data Assimilation over Global Oceans, *J. Geophys. Res.*, Vol.113, DOI: 1029/2007JD009065, 2008
- Zhang, R., G. Li, J. Fan, D. L. Wu, and M. J. Molina, (2007), Intensification of Pacific Storm Track Linked to Asian Pollution, *PNAS* | March 27, 2007 | Vol.104 | no. 13 | 5295-5299.